

## HIGHER OXIDATION STATE MANGANESE BIOMOLECULES

JOHN B. VINCENT and GEORGE CHRISTOU

Department of Chemistry, Indiana University,  
Bloomington, Indiana 47405

- I. Introduction
- II. Superoxide Dismutase
  - A. The Native System
  - B. Model Studies
- III. Acid Phosphatase
  - A. The Native System
  - B. Model Studies
- IV. Transferrin
  - A. The Native System
  - B. Model Studies
- V. Catalase
  - A. The Native System
  - B. Model Studies
- VI. Photosystem II
  - A. The Native System
  - B. Model Studies
  - C. Proposed Mechanisms for Water Oxidation
- VII. Concluding Remarks
- References

### I. Introduction

There is no doubt that the various biological molecules (biomolecules) known to contain tightly bound manganese (Mn) atoms represent an area of intense investigation at the present time. These studies have been directed toward the elucidation of the structure, properties, and mode of function of these systems, and a variety of techniques have been employed in attempting to attain these objectives, including X-ray crystallography, electron paramagnetic resonance (EPR), nuclear magnetic resonance (NMR), and extended X-ray absorption fine structure (EXAFS) and edge (XANES) studies. As more

data have become available, these have also stimulated intense interest within the inorganic chemistry community, and many groups are actively involved in attempting to synthesize inorganic Mn complexes which represent synthetic models of the native Mn sites. The latter effort is an important component of the overall interdisciplinary effort, for it can provide structural detail to a precision not possible for the large biomolecules and even reproduction of the biological substrate transformation using completely synthetic materials, with potential for deduction of the mechanism of action. In planning the scope of this survey, we have felt it would be an important contribution to cover all these aspects of the continuing interdisciplinary effort. For this reason, we have not aimed for an exhaustive review of either Mn biochemistry or Mn inorganic chemistry, but for a hybrid to straddle both areas. More detailed and exhaustive reviews of Mn biochemistry and the inorganic chemistry of Mn are, in any case, already available elsewhere in separate form in the literature. For this reason, we have also concentrated on those systems containing higher oxidation state Mn ( $>II$ ), systems which represent the primary area of current effort by both the biochemistry and inorganic chemistry communities. This article covers the literature up to mid-1987, but has also included unpublished work when it has been available to the authors.

## II. Superoxide Dismutase

### A. THE NATIVE SYSTEM

The first discovered manganese(III) metallobiomolecule was a superoxide dismutase isolated from the aerobic bacterium *Escherichia coli*, reported in 1970 (1). Since its isolation Mn superoxide dismutase (SOD) has been extensively studied (38, 39). Mn SOD enzymes have been isolated and characterized from sources belonging to all five kingdoms of living beings. Sources include, in addition to *E. coli*, pea leaves (5), the prokaryotic microorganism *Acholeplasma laidlawii* (6), the thermophilic bacteria *Thermus aquaticus* (7) and *Thermus thermophilus* (8), the purple bacterium *Rhodospseudomonas spheroides* (9), the fungus *Pleurotus olearius* (10), yeast (11), *Streptococcus mutans* (12), *Bacillus stearothermophilus* (13), and the liver of chicken (14), rat (15), bullfrog (16), and man (17).

The stoichiometry of Mn SOD enzymes varies greatly. Whereas the *E. coli* enzyme is a dimer, SOD enzymes from a number of sources, such as *T. thermophilus* (8) and chicken liver (14), are tetrameric. Each subunit, however, is consistently about 20 kDa, despite the number of

subunits present. Also, some discrepancy appears in the number of manganese atoms present for each dimeric unit. A number of enzymes possess a stoichiometry of one metal per subunit while others appear to contain half this number (Table I). The *Pisum sativum* enzyme appears to possess only one Mn atom, despite having a molecular weight of 94,500 (20). While loss of manganese may be a problem in some cases, rebinding experiments confirmed the metal content found for this isolated protein. A SOD from *Nocardia asteroides* has been isolated which contains one to two atoms of Mn, Fe, and Zn (32).

While the stoichiometries of the Mn SOD enzymes appear to vary, the properties of the Mn-binding site do not. This is borne out in the electronic spectra of these proteins, which display a great degree of similarity despite the diversity of sources from which they have been isolated (Table II). This type of spectrum is distinctive for manganese in the trivalent oxidation state (3). The native enzymes are EPR silent, as might be anticipated if they contained Mn solely as the trivalent ion ( $S = 2$ ) (1, 6, 12, 18–20, 24). However, when the enzymes are denatured, the characteristic six-line pattern of Mn(II) ( $I = 5/2$ ) appears. Magnetic susceptibility studies with the *E. coli* SOD were consistent with the presence of a monomeric Mn(III) complex with a zero-field splitting of 1 to 2  $\text{cm}^{-1}$  (4). The enzymes are additionally metal specific (however, see Refs. 36 and 37); metal reconstitution studies with *E. coli* and *B. stearrowthermophilus* revealed a strict requirement for Mn for superoxide dismutase activity (2, 22, 23).

Preliminary X-ray crystallographic studies have appeared on several Mn SOD enzymes (27–29). The crystal structure of the *T. thermophilus* enzyme at 4.4 Å resolution (27) indicated a high degree of homology between the secondary and tertiary structure of the Mn enzyme and an iron SOD isolated from *E. coli* (3.1 Å resolution) (33). Each possesses a single metal-binding site per subunit. Sequence homologies between the

TABLE I  
STOICHIOMETRY OF Mn SUPEROXIDE DISMUTASES

Source	Mn	Subunits	MW/subunit	Reference
<i>Escherichia coli</i>	1.6–1.8	2	21,600	1
<i>Acholeplasma laidlawii</i>	1.02	2	21,600	6
<i>Rhodopseudomonas spheroides</i>	1.08–1.12	2	18,400	9
<i>Thermus aquaticus</i>	2.12	4	21,000	7
Bovine heart	2	4	20,700	30
Bullfrog liver	4	4	22,000	16
Yeast	3.8	4	25,000	11

TABLE II  
VISIBLE SPECTRA OF Mn SUPEROXIDE DISMUTASES

Source	$\lambda_{\max}$ (nm) <sup>a</sup>	Reference
Bullfrog liver	475(625), 600(sh)	16
<i>Escherichia coli</i>	473(200)	1
<i>Pisum sativum</i>	480(sh), 600(sh)	5, 26
<i>Acholeplasma laidlawii</i>	450	6
<i>Thermus aquaticus</i>	478, 600(sh)	7
<i>Rhodopseudomonas spheroides</i>	475(542)	9
<i>Thermus thermophilus</i>	480(910), 600(sh)	8
<i>Pleurotus olearius</i>	475(438), 600(sh)	10, 31
Yeast	460	11
Chicken liver	475(584), 600(sh)	14
<i>Streptococcus mutans</i>	473(280)	12
Red algae	450(170)	21
Human liver	480(513), 600(sh)	17
<i>Mycobacterium</i> sp.	475(118)	24
<i>Paracoccus denitrificans</i>	470(sh), 600(sh)	25

<sup>a</sup> Data in parentheses are  $\epsilon_M/\text{Mn}$ .

two forms of SODs have been appreciated for some time (34). Closer scrutiny of the partial sequences combined with the X-ray data implicated three histidine residues and one aspartate residue as metal ligands (27, 35). Interestingly, the presence of ferrous iron has been shown to have an effect on Mn SOD biosynthesis (36), and recently superoxide dismutases have been isolated which are active with either metal (19, 37).

Refinement of the X-ray structural studies on *T. thermophilus* to 2.4-Å resolution has allowed resolution of the metal ligation (40). The structure of the manganese-binding site is shown in Fig. 1. Only four atoms from the protein appear to be binding the Mn(III): three imidazole nitrogens from histidine residues 28, 83, and 169 and a single carboxylate oxygen from aspartate 165. A fifth coordination site appears to be filled by a molecule of water, imparting overall trigonal bipyramidal geometry about the manganese center. Nuclear magnetic resonance relaxation rate studies on the *E. coli* enzyme had previously implicated one molecule of water as a possible manganese ligand (41). The five-coordinate manganese complex bearing a +2 charge sits in an apolar environment (40). Careful analysis of the structural data indicated a cavity is present between His 83 and His 169, adjoining the manganese. Such a cavity could be a substrate-binding site, such that an inner-sphere Mn superoxide complex could form without dissociation

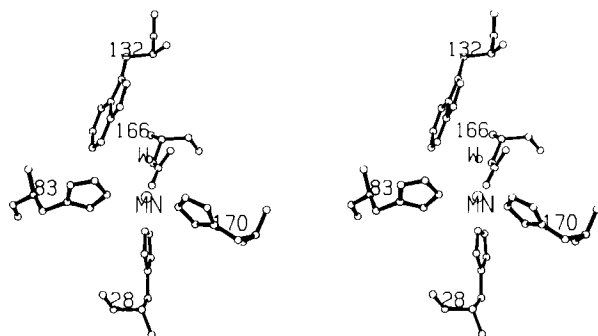


FIG. 1. Stereo figure of the Mn(III) environment in Mn SOD from *Thermus thermophilus*. The coordinates were derived from partial refinement of data at 1.8-Å resolution. (Dr. M. L. Ludwig, personal communication.)

of the coordinated  $\text{H}_2\text{O}$  molecule. This would be consistent with the rapid kinetics of the superoxide dismutation (55, 56). Additionally, five-coordinate Mn(III) coordination complexes are quite uncommon, being limited almost exclusively to compounds with softer ligands such as chloride (42, 43) or thiolate (vide infra). The shortest  $\text{Mn}\cdots\text{Mn}$  distance in the enzyme was determined to be about 18 Å (40).

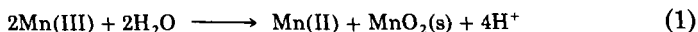
The four protein residues which serve as metal ligands are conserved in the amino acid sequences of all Mn SODs completely sequenced to date [i.e., *T. thermophilus* (44), yeast (45), *E. coli* (46), human liver (47), and *B. stearothermophilus* (48)]. [The DNA sequence of the *E. coli* Mn SOD gene and mouse Mn SOD gene have also recently been determined (49, 59).] Thus, it seems quite probable that the Mn-binding site structure is analogous (or nearly so) in all Mn SODs. Further support for this comes from EPR studies of the Cu(II)-substituted *B. stearothermophilus* enzyme, which indicate the presence of three imidazole ligands in a rhombic metal complex (50).

Other than in prokaryotic cells which lack mitochondria and chloroplasts, manganese superoxide dismutases are apparently restricted to the above two organelles in eukaryotic cells (51, 52); this forms strong support for the symbiotic hypothesis for the origin of mitochondria and chloroplasts (53, 54). Kinetic studies of superoxide dismutation by these enzymes indicate three oxidation states of Mn (presumably divalent, trivalent, and tetravalent) are involved in the catalytic cycle (57, 58). They also show that a  $\text{Mn}-\text{O}_2^-$  complex may conceivably be formed. Well-characterized Mn-dioxygen (i.e.,  $\text{O}_2$ ,  $\text{O}_2^-$ ,  $\text{O}_2^{2-}$ ) adducts are extremely rare, the first structurally characterized example being reported only in 1987 (60).

## B. MODEL STUDIES

Structurally characterized trivalent manganese imidazole or imidazolate complexes are also extremely rare. Current examples are limited to Mn(III) porphyrins (61), Mn(III) thiolates (Section III,B), a Mn(III) salicylate complex (Section IV,B) and Mn(III) and Mn(IV) carboxylate complexes (Section VI,B) (62). None of these complexes contains a Mn-to-imidazole ratio greater than two; consequently, no structural model for Mn SOD exists presently in Mn coordination chemistry. However, a five-coordinate Mn(II) monomer with three imidazole ligands,  $\text{Mn}(2\text{-Me-ImH})_3\text{Cl}_2$  (ImH = imidazole), has been characterized by X-ray diffraction techniques (63).

Carboxylic acids have long been used to stabilize trivalent manganese in aqueous media, as disproportionation is slowed by the presence of  $\text{H}^+$  [Eq. (1)]. Carboxylate functionalities have often been incorpo-

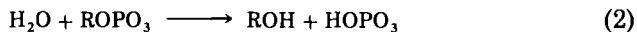


rated into multidentate ligands aimed at stabilizing higher oxidation state manganese.  $\text{Mn}^{2+}$  complexes of a number of these ligands have been shown to serve as catalysts for superoxide dismutation; however, the catalytic rate constants for these systems are orders of magnitude slower than the enzymatic rate (64–66). Synthesis of satisfactory model systems and their use to mimic the enzyme function thus represent areas warranting further study.

## III. Acid Phosphatase

### A. THE NATIVE SYSTEM

The isolation of the first manganese-containing acid phosphatase was reported in 1971 from the juice of the sweet potato (Kokei No. 14) (67). The enzyme was unique in that it was distinctly purple, the color resulting from a broad absorption band with a maximum at 555 nm. The enzyme was determined to be 110 kDa, composed of two 55-kDa subunits. The purple enzyme was capable of hydrolyzing a variety of biologically relevant phosphates as well as inorganic pyrophosphate [Eq. (2)]. Emission spectroscopy revealed the presence of Mn (68).



Comparison of the visible spectrum with those of reported Mn SODs led

the authors to speculate the purple color resulted from a manganese chromophore.

The sweet potato enzyme could be inactivated by *o*-phenanthroline and 2,2'-bipyridine; the activity could be restored by the addition of  $\text{Zn}^{2+}$  and partially by added  $\text{Mn}^{2+}$  or  $\text{Co}^{2+}$  (69). The amino acid composition revealed an usually large content of tyrosine. Later experiments were able to quantitate the amount of Mn present at two Mn per mole enzyme (70). Additionally, the native enzyme was shown to be EPR inactive; however, treatment of the enzyme with acid led to the appearance of a six-line pattern typical of aqueous  $\text{Mn}^{2+}$  coincident with the loss of the purple color, further evidence for the association of Mn with the 555-nm absorbance band.

Similar Mn-containing enzymes were subsequently isolated from other plant sources: spinach leaves (71), rice plant cultured cells (72), soybeans (73–75), and the tubers of the sweet potato Kintoki (76–81) (Table III). Sweet potatoes have recently been reported to possess two different acid phosphatases which were immunologically distinct but which have similar molecular weights and metal content (106). Interestingly, sulfhydryl reagents have been shown to inactivate the soybean enzyme (75).

Presently, the vast majority of information on the Mn site in these acid phosphatases comes from the enzyme from sweet potato tubers. This 110-kDa enzyme is identical to the previously reported sweet potato enzyme; likewise, a 55-kDa subunit was found (78). However, the enzyme possesses only one Mn per enzyme molecule. At 293 and 77 K, no EPR signal could be detected for the native enzyme. Inactivation of the enzyme by heat treatment or the addition of acid results in the appearance of a six-line EPR pattern due to aquated Mn(II). As in the case of Mn SODs, this was taken as evidence for Mn(III) in the native

TABLE III  
Mn ACID PHOSPHATASES

Source	MW	Subunit MW	$\lambda_{\text{max}}$ (nm)	Total Mn
Sweet potato <sup>a</sup>	110,000	55,000	555	2
Sweet potato <sup>b</sup>	110,000	55,000	515	1
Spinach	92,000	46,000	530	?
Rice <sup>c</sup>	65,000	65,000	560	?
Soybean	240,000	60,000	540	?

<sup>a</sup> Kokei.

<sup>b</sup> Kintoki.

<sup>c</sup> Major isoenzyme.

state. The violet enzyme gave an absorbance maximum at 515 nm with  $\epsilon = 2460 \text{ M}^{-1} \text{ cm}^{-1}$ . Based on circular dichroism spectra, this band was assigned to a ligand-to-Mn(III) charge transfer band. The resonance Raman spectra of the native enzyme, when excited by the 5745-Å line of an argon laser, exhibited prominent lines at 1230, 1298, 1508, and  $1620 \text{ cm}^{-1}$  (76). The spectra are strikingly similar to those of synthetic iron-phenoxide complexes (97), uteroferrin (98), and Mn-transferrin and Fe-transferrin (Section IV,A), where these bands have been assigned to vibrations of a phenoxide ligand(s) coordinated to the metal. If the background fluorescence from tryptophan residues is quenched, the resonance Raman spectra contains an enhanced band at  $370 \text{ cm}^{-1}$  (77). The authors assigned this band to a Mn(III)-S stretching mode based on comparison with the Raman spectra of a Mn(III) dithiocarbamate complex (89) and iron-sulfur proteins (99). These studies confirm that the 515-nm band results from tyrosine  $\rightarrow$  Mn charge transfer transitions and may have contributions from a cysteine  $\rightarrow$  Mn transition. The presence of a Mn(III)-thiolate interaction is likewise supported by cysteine determinations that indicate no free sulfhydryl groups are present in the native enzyme, but 1 mol of  $-\text{SH}$ /mol of enzyme is present in denatured enzyme (78).

Recently, spectroscopic studies and metal substitution experiments have been utilized to investigate directly the active site of the enzyme.  $^{19}\text{F}$  nuclear magnetic resonance studies and proton relaxation rate measurements revealed that inhibitors such as  $\text{F}^-$  interact directly with the paramagnetic center (79). Likewise, the  $^{31}\text{P}$  NMR signal of the enzyme-phosphate complexes was substantially broadened, indicating coordination to the manganese site (80, 81). Substitution of the Mn with Fe resulted in a shift of the visible absorption band to 525 nm ( $\epsilon = 3000 \text{ M}^{-1} \text{ cm}^{-1}$ ) coincident with reduction of phosphate ester hydrolysis activity to approximately 53%. EPR spectra of the iron-substituted enzyme displayed a signal at  $g = 4.39$ , typical of high-spin Fe(III). Satisfactory substitutions were not possible with  $\text{Zn}^{2+}$  or  $\text{Cu}^{2+}$  (79). Chemical modification of a histidine residue has been shown to cause a reduction in activity of 96% (81). Protecting the residue resulted in no loss of activity. The pH profile of the inactivation rates of the enzyme showed an amino acid residue having a  $\text{p}K_a$  of  $\sim 7.2$  was involved in the inactivation. Thus, the authors concluded that at least one histidine residue per enzyme subunit participates in the catalytic function of the acid phosphate and may indeed serve as a ligand to Mn(III).

The presence of Mn in the naturally occurring acid phosphatase has been questioned (82). The electronic spectra of these plant enzymes are extremely similar to those of mammalian enzymes which contain two



atoms of Fe. Likewise, resonance Raman studies do not differentiate between metal centers, isostructural Fe and Mn complexes giving essentially identical spectra. Indeed, studies of a purple acid phosphatase from red kidney bean have indicated the presence of two atoms of Fe and two atoms of Zn per mole enzyme (83). The visible absorption spectra showed a maximum at 560 nm with  $\epsilon = 3360 \text{ M}^{-1} \text{ cm}^{-1}$ . The plant enzyme is composed of two subunits of 55 kDa, identical to the sweet potato enzymes; the amino acid composition of the enzyme is remarkably similar to the earlier reported Mn enzyme. Very recently, a purple acid phosphatase from sweet potato has been isolated which contains two atoms of Fe per mole enzyme (84). The physical properties of the enzyme are remarkably similar to the Mn enzyme, but the Fe version has >10-fold higher specific activity. Thus, the status of Mn acid phosphatase is uncertain at the present time. Perhaps a situation similar to Mn SODs and Fe SODs also exists with these enzymes, viz. both Mn and Fe forms may exist.

## B. MODEL STUDIES

The proposed presence of a Mn(III)–cysteine linkage in Mn acid phosphatase has spurred investigations into the synthesis of Mn(III) thiolate complexes and into how such a couple—a strong oxidizing agent and good reducing agent—can be stabilized. Structurally characterized high-valent Mn complexes with sulfur-based ligation are uncommon, being limited to thiocyanates (85), dithiolenes (86), dithiocarbamates (87–90), and chelating thiolates (91–96).

In 1983, two independent laboratories reported the synthesis and structural characterization of the first true Mn(III)–thiolate (91, 92). Aerial oxidation of an alcoholic solution of  $\text{MnCl}_2 \cdot 4\text{H}_2\text{O}$ ,  $\text{Na}_2(\text{edt})$  ( $\text{edt}$  = ethane-1,2-dithiolate), and cation resulted in the formation of a deep green-colored solution from which dark green crystals of  $[\text{NEt}_4]_2[\text{Mn}_2(\text{edt})_4]$  precipitated. The ability of the ligand to form this air- and water-sensitive compound probably stems from the bidentate nature of the ligand, which forms a five-membered chelate ring on complexation. The chelate effect inhibits disulfide formation, presumably the most facile route for decomposition of the complex. Solution studies indicate that the dimer partially dissociates in acetonitrile and, in strongly coordinating solvents, dissociates completely to give a solvated monomeric species (92, 101). This behavior in solution has been exploited by showing that the addition of imidazole to dimethylformamide solutions of the dimer results in the formation of the five-coordinate monomer  $[\text{NMe}_4][\text{Mn}(\text{edt})_2(\text{ImH})]$  (93, 94). The manganese center is in a distorted square pyramidal environment with the bound

imidazole in the axial position. Employment of NaIm results in the formation of the complex  $[\text{NEt}_4]_3[\text{Mn}_2(\text{edt})_4(\text{Im})]$  (95). The structure of the anion is shown in Fig. 2. This compound represents the first discrete imidazolate complex of Mn(III). While this type of coordination has not been found in nature for Mn (to date), it has been firmly established in Co,Zn superoxide dismutases (102). Additionally, other multinuclear, homoleptic manganese(III) thiolates have since been synthesized and structurally characterized (95, 103). The synthesis of an unstable monodentate thiolate-Mn(III) complex  $[\text{PPh}_4][\text{Mn}(\text{S-2,4,6-}i\text{-Pr}_3\text{-C}_6\text{H}_2)_4]$  has recently been reported (100); use of this bulky thiolate was designed to sterically hinder disulfide formation and reduction of manganese. However, thermal instability of the purple crystals prevented structural characterization.

While  $\text{Mn}(\text{edt})_2(\text{ImH})^-$  is monomeric and contains thiolate and imidazole ligation (as may occur in the purple acid phosphatase enzyme), the visible spectra of the complex and the other synthetic bidentate thiolate complexes distinctly differ from that of the enzyme. The monodentate thiolate complex is, however, purple in solution (100), but the visible spectrum of this complex was not reported.

Recently, a Mn(III) complex with mixed O-, N-, and S-based ligation and its Fe(III) analog have been synthesized (96).  $\text{Mn}(\text{thiosalicylate})_2(\text{ImH})^-$  (Fig. 3) is a five-coordinate, square pyramidal monomer with *cis*-thiolate sulfurs and the imidazole ligand in the axial position, analogous to the edt monomer. The Fe analog,  $\text{Fe}(\text{thiosalicylate})_2(2\text{-Me-ImH})^-$ , is trigonal bipyramidal with an axial oxygen; the different

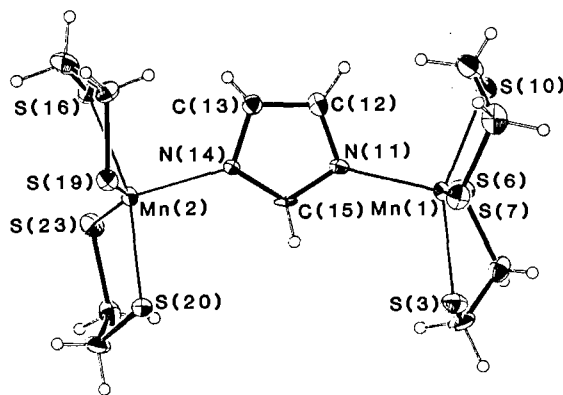


FIG. 2. The structure of  $[\text{Mn}_2(\text{edt})_4(\text{Im})]^{3-}$ . (Reproduced with permission from Ref. 95. Copyright 1985, American Chemical Society.)

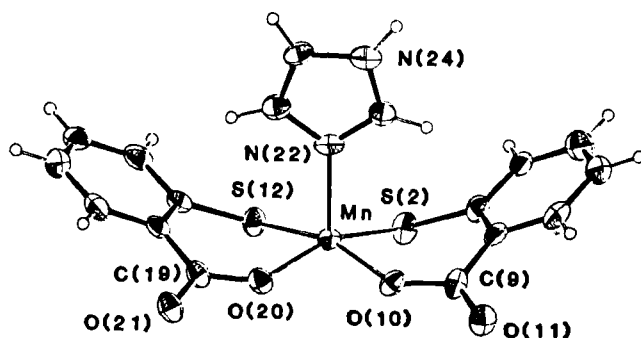


FIG. 3. The structure of  $[\text{Mn}(\text{thiosal})_2(\text{ImH})]^-$ . (Reproduced with permission from Ref. 96. Copyright 1985, American Chemical Society.)

geometry is presumably the result of the bulkier substituted imidazole. The visible spectra of the complexes are quite similar to those of the enzyme and the Fe-substituted enzyme (Table IV). In both cases, the spectra are red shifted for the Fe analogs. The intense visible bands for the synthetic complexes were assigned to thiolate  $\rightarrow$  metal charge transfer bands, as analogous bands are not found in Mn(III) salicylate and imidazole complexes. The authors thus concluded that mixed O, N, and S ligation is required before spectral characteristics of the native enzyme are approached, suggesting a similar situation may exist in the enzyme.

Unfortunately, no infrared or Raman data on these Mn(III)-thiolates have yet been reported, making comparisons with the enzyme difficult. Mn-transferrin and Fe-transferrin have Raman bands in the region between 340 and 370  $\text{cm}^{-1}$  (104); indeed, Sugiura *et al.* could not exclude the possibility that the  $\sim 370 \text{ cm}^{-1}$  band might actually arise from a

TABLE IV  
VISIBLE SPECTRA DATA FOR  
ACID PHOSPHATASES AND  
MODEL COMPLEXES

Complex/enzyme	$\lambda_{\text{max}}$ (nm) <sup>a</sup>
$[\text{Mn}(\text{thiosal})_2(\text{ImH})]^-$	450(2760), 500(2500)
$[\text{Fe}(\text{thiosal})_2(2\text{-MeImH})]^-$	565(5070)
Sweet potato (Kintoki)	515(2460)
Fe substituted	525(3000)

<sup>a</sup> Data in parentheses are  $\epsilon_M$ .

Mn–O (phenoxide) stretch (78). Again, the lack of infrared and Raman data on Mn(III) phenoxides precludes any firm conclusions (105).

#### IV. Transferrin

##### A. THE NATIVE SYSTEM

Transferrin is a reversible iron-binding protein found in vertebrate blood serum, in egg white (conalbumin or ovotransferrin), and in mammalian milk and other physiological fluids (lactoferrin). The primary function of the serum enzyme is iron transport, although a number of other functions, such as radical scavenging, have been suggested. The other forms of the protein appear to serve as iron scavengers, removing iron available for the growth and development of microorganisms. All of these proteins consist of a single approximately 80-kDa polypeptide. Two metal-binding sites are present per molecule of protein, which binds iron exclusively in the trivalent state. Binding occurs only when a suitable anion (probably carbonate or bicarbonate in the native protein) is concomitantly bound. Recently, the two binding sites have been shown to be inequivalent. Transferrin in the natural system is normally maintained at 30% saturation (for reviews, see Refs. 107–110).

The structure of human milk transferrin has very recently been determined crystallographically at a resolution of 3.2 Å (111). The polypeptide has approximate twofold symmetry. Both the C- and N-terminus halves form globular lobes, with each possessing one iron-binding site. Consequently, 42 Å separate the iron sites. The three-dimensional structure of one of the iron-binding sites is shown in Fig. 4. Both irons possess almost identical coordination spheres. The protein provides four metal ligands: one histidine residue, two tyrosine residues, and one aspartate residue. Tyrosine and histidine had been implicated as ligands by previous spectroscopic and chemical modification studies (112–115). The remaining two coordination sites, disposed cis to one another, appear to contain the bicarbonate anion and/or water molecules, as previously indicated by NMR relaxation rate experiments (116, 117).

Inman first showed that trivalent manganese formed a complex with transferrins by adding hydrogen peroxide to a mixture of  $\text{Mn}^{2+}$  and the apoenzyme (118). Displacement studies revealed that the order of binding for both the human serum enzyme and ovotransferrin was  $\text{Fe}^{3+} > \text{Mn}^{3+} > \text{Cu}^{2+}$ . The Mn complex displayed a distinctive visible band maximum at 429 nm. Further studies of the Mn-containing protein by

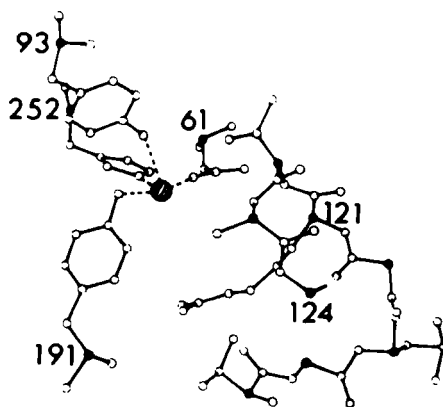


FIG. 4. The iron coordination in lactoferrin at 3.2-Å resolution. (Reproduced from Ref. 111 with the authors' permission.)

rotary dispersion titration indicated two ions of Mn bind to each molecule of protein (119). The Mn(III) complex gave rise to positive Cotton effects very similar to the Fe-containing protein. Aisen *et al.* have shown unequivocally by magnetic susceptibility measurements that transferrin tightly binds Mn exclusively in the trivalent state (120). While one anion was found for each of the two Mn ions, binding of the higher valent Mn did not require peroxide. Under anaerobic conditions, the deep brown color of the Mn(III) complex developed more slowly than in the presence of air, indicating that O<sub>2</sub> could serve as a suitable oxidizing agent for the divalent Mn. Difference ultraviolet spectra between the apoprotein and the manganese-containing protein illustrate that a band at 255 nm is enhanced on Mn binding, typical of metals binding to tyrosine (121). Additional evidence for Mn(III) binding versus Mn(II) binding comes from fluorescence studies. The enzyme possessing tightly bound Mn(III) exhibits substantial fluorescence quenching. In the presence of divalent manganese a lesser degree of quenching is exhibited, which increases with time or the addition of peroxide (122).

Excitation of the visible absorption band of the manganese-containing proteins of human serum transferrin and ovotransferrin with an argon laser results in resonance-enhanced Raman bands at 1603, 1501, 1264, 1173, and 752 cm<sup>-1</sup> and 1600, 1500, 1236, 1171, and 752 cm<sup>-1</sup>, respectively (104). These frequencies are almost identical to those enhanced in the iron analog, demonstrating that the Mn probably occupies the iron-binding sites. All of these enhanced bands were assigned to phenolic vibrational modes. Similar studies with human

TABLE V  
RESONANCE RAMAN-ENHANCED BANDS OF TRANSFERRINS

Protein	Mn(III)	Fe(III)
Ovotransferrin	1600, 1500, 1236, 1171, 752	1605, 1504, 1270, 1250, 1170, 759
Human serum transferrin	1603, 1501, 1264, 1173, 752	1605, 1504, 1281, 1260, 1177, 759
Human lactoferrin	1601, 1499, 1462, 1253, 1169	1604, 1500, 1447, 1272, 1170, 1004, 939

lactoferrin gave almost identical results (see Table V) (122). Additionally, an intermetal distance of  $35.5 \pm 4.5$  Å has been determined from energy transfer between an excited terbium ion in one binding site and a Mn(III) ion in the other for human serum transferrin (123).

A biological role for Mn transferrin has been demonstrated during the last two decades. Keefer and co-workers reported in 1970 that transferrin was the protein component of rat blood serum that binds Mn (124). A single protein in the serum bound the majority of both Mn and Fe in a double-labeling experiment and of Mn in experiments with only the one metal. Immunoelectrophoresis indicated this protein corresponded to transferrin. Similar studies with human serum also demonstrated the *in vitro* binding of manganese by transferrin (125, 126). *In vivo* studies with rabbits injected with  $^{54}\text{Mn}$  detected transferrin with bound  $^{54}\text{Mn}$  (125). When divalent manganese in various forms and Mn-transferrin were injected into the blood of goats and cows, the divalent Mn was rapidly and efficiently removed from the blood by the liver (126). The trivalent Mn associated with the transferrin, however, was not rapidly removed. The small fraction of Mn absorbed when only  $\text{Mn}^{2+}$  was used behaved in an identical manner to the Mn(III)-transferrin complex. These results have led to the conclusion that much of the Mn not initially removed by the liver is transported to the tissues primarily as Mn-transferrin (125, 127).

## B. MODEL STUDIES

The manganese(III)-phenoxide couple is quite unstable; in organic chemistry, Mn(III) and Mn(IV) complexes have been demonstrated to be excellent oxidants for phenols and their analogs (145). Indeed, a peroxidase isolated from white rot fungus is dependent on extracellular Mn(II) (146-149). The heme-peroxide moiety of this enzyme is reduced by the Mn, which in turn (as the trivalent species) migrates to the phenolic substrate. The substrate is thus oxidized by the generated

Mn(III). Structurally characterized higher valent manganese complexes with phenoxide-type ligation are limited to Mn(III) and Mn(IV) Schiff base complexes (128–135), Mn(III) and Mn(IV) catecholates (136–139), Mn(III) and Mn(IV) salicylates (140–142), and Mn(III) biphenoxides (143). However, of these ligands, only biphenoxide is similar electronically to tyrosine; Mn(III) complexes of these ligands, in general, lack the intense phenoxide  $\rightarrow$  metal charge transfer band centered at  $\sim 435$  nm.

It has been shown that reaction of  $\text{Mn}_3\text{O}(\text{O}_2\text{CPh})_6(\text{py})_2(\text{H}_2\text{O})$  with  $[\text{NEt}_3\text{H}]_2(\text{biphenoxide})$  results in the formation of  $[\text{Mn(III)(biphen)}_2(\text{biphenH})]^{2-}$  (biphen = 2,2'-biphenoxide) (Fig. 5) (143). The complex is a rare example of five-coordinate Mn(III) without softer ligands such as thiolate or chloride. The monodentate biphen–Mn bond represents the first stable example of the Mn–phenoxide couple. The monomer displays several intense absorption bands (Table VI). In DMSO (where the compound may be six coordinate), a band at 430 nm, very similar to that of the enzyme, is assigned to a phenoxide  $\rightarrow$  Mn(III) charge transfer band.

Reaction of the monomer with 2,2'-bipyridine results in the formation of the mixed-valence dimer,  $\text{Mn}_2(\text{III,II})(\text{biphen})_2(\text{biphenH})(\text{bipy})_2$

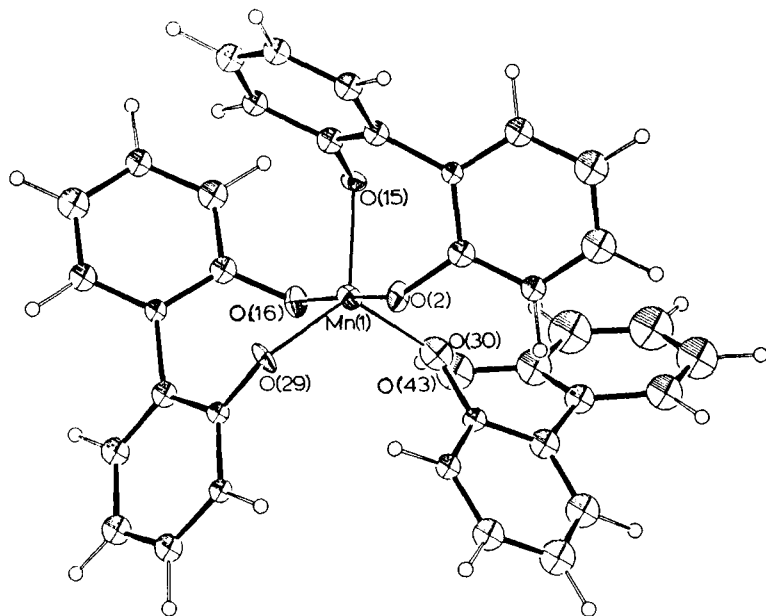
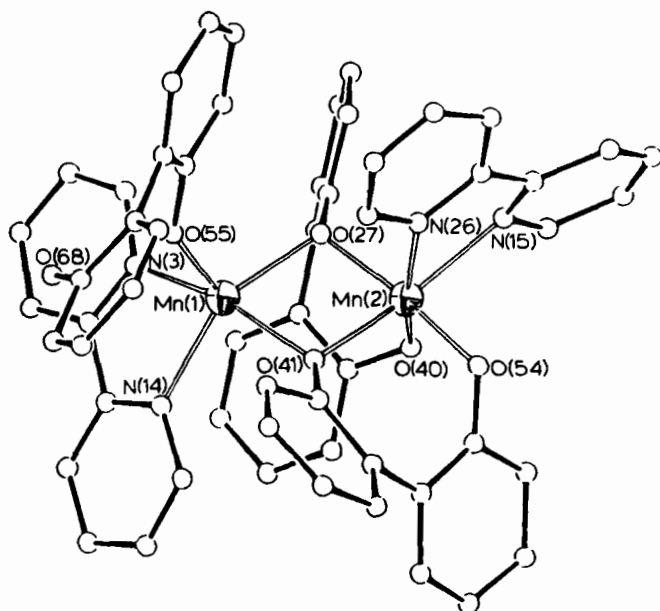


FIG. 5. The structure of  $[\text{Mn}(\text{biphen})_2(\text{biphenH})]^{2-}$ .

TABLE VI

UV/VISIBLE SPECTRA OF Mn TRANSFERRINS AND MODEL COMPLEXES

Complex/protein	Solvent	UV/visible $\lambda_{\max}$ (nm) <sup>a</sup>
Mn(biphen) <sub>2</sub> (biphenH) <sup>2-</sup>	CHCl <sub>3</sub>	242(38, 650), 282(24, 660), 380(sh, 3115), 490(2260), 665(sh, 1115)
	DMSO	430(2950)
Mn <sub>2</sub> (biphen) <sub>2</sub> (biphenH)(bipy) <sub>2</sub>	CH <sub>2</sub> Cl <sub>2</sub>	240(33, 200), 283(32, 100), 306(9, 960), 390(2030), 453(1930), 642(830)
Human lactoferrin <sup>b</sup>	H <sub>2</sub> O	295, 340(4475, sh), 435(4810), 520(4850, sh), 640(2310, sh)
Ovotransferrin <sup>c</sup>	H <sub>2</sub> O	430(4000)

<sup>a</sup> Data in parentheses are  $\epsilon$ /Mn(III).<sup>b</sup> Ref. 121.<sup>c</sup> Ref. 104.FIG. 6. The structure of  $[\text{Mn}_2(\text{biphen})_2(\text{biphenH})(\text{bipy})_2]$ .



(Fig. 6). The dinuclear complex displays an intense absorption band in its visible spectra. [The Mn(II) is not expected to contribute significantly to the visible spectrum, as Mn(II)(phenoxide)<sub>2</sub> is an amorphous, white polymer (144)]. These two complexes represent the first well-characterized high-valent Mn-phenoxide complexes. Note also that in the structures of the biphenoxide complexes, the benzene rings of each half of the biphenoxide ligands are oriented such that no conjugation is present and each half of the ligand is similar, electronically, to phenoxide.

The fact that the four metal ligands provided by the transferrin apoprotein involve three different amino acid residues, i.e., histidine, tyrosine, and aspartate, is most interesting. Inorganic mononuclear complexes with such a variety of ligand types are not often encountered; however, a Mn(III) complex with imidazole, carboxylate-, and phenoxide-type ligation has been structurally characterized. The complex [Mn(sal)<sub>2</sub>(ImH)<sub>2</sub>]<sup>-</sup> (Fig. 7) (sal = salicylate) possesses two trans imidazoles and two salicylates disposed trans to one another (142).

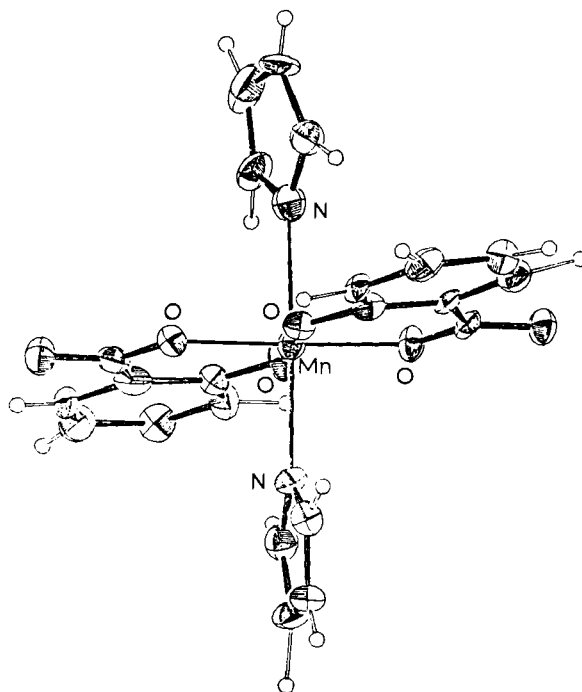


FIG. 7. The structure of [Mn(sal)<sub>2</sub>(ImH)<sub>2</sub>]<sup>-</sup>.

## V. Catalase

## A. THE NATIVE SYSTEM

The bacterium *Lactobacillus plantarum* and its closest allies are unusual in that they are aerobic organisms but do not produce a superoxide dismutase. This bacterium instead accumulates Mn(II) to an intramolecular level on the order of 25 mM (150–152). *In vitro* studies indicated that Mn(II) formed a complex with lactate which possessed significant superoxide activity (153). These bacteria are additionally unable to produce heme and, consequently, when grown in the absence of heme, produce a hemeless catalase, or “pseudocatalase” (154–158). Unlike heme-containing catalases, the enzyme is not inhibited by cyanide or azide, and the addition of either Mn or Fe into the growth medium increased the amount of the pseudocatalase present. However, neither of the metals could be detected in partially purified enzyme assays (157).

In 1983, Kono and Fridovich reported the isolation of a pseudocatalase from *L. plantarum* which contained manganese (159). The enzyme was 172 kDa; the original report gave a subunit of 28.3 kDa and  $1.12 \pm 0.37$  atoms of manganese per subunit. The visible spectrum of the enzyme displayed an absorption maximum at 470 nm ( $\epsilon = 1.35 \times 10^3 \text{ M}^{-1} \text{ cm}^{-1}$ ) with shoulders at 398 and 500 nm. This spectrum is extremely similar to those of Mn superoxide dismutases (Section II,A) and, thus, indicative of the presence of Mn(III). Comparison of the amino acid compositions of the two enzymes suggested that they are not closely related. The pseudocatalase possessed no superoxide dismutase activity but had a turnover number of  $3.9 \times 10^5$  mol of peroxide per mole of enzyme per second.

Subsequent studies of the manganese catalase demonstrated its biological utility (160). Hydroxylamine-treated bacteria, with the Mn catalase irreversibly inactivated, were sensitive to the lethality of 5 mM  $\text{H}_2\text{O}_2$  in the stationary phases of growth, unlike the untreated bacteria. The catalytic cycle of the pink enzyme was also investigated by inhibition and reactivation studies (161). The enzyme was inactivated by  $\text{NH}_2\text{OH}$  and  $\text{H}_2\text{O}_2$  but was not inactivated by either reagent separately. Approximately 40% of the activity lost by the addition of the two reagents could be restored by dithionite or superoxide. Other tested reductants could not restore activity. Oxidants tested also failed to reactivate the enzyme. The active enzyme lost apparently one-half of its activity when exposed to a flux of  $\text{O}_2^-$ .

Improved purification procedures were subsequently developed for the manganese catalase (164). While the enzyme from this preparation

was again found to be 172 kDa, the subunit was 34 kDa, making the enzyme a rare homopentamer. Between 9 and 12 atoms were present per mole of enzyme. Amino acid analyses indicated that no cysteine was present. These observations led the authors to speculate that each subunit might possess a dinuclear manganese assembly.

Subsequently, a manganese-containing catalase has been isolated from the aerobic bacterium *Thermoleophilum album* (162). The enzyme is 141 kDa and is composed of four subunits of 34 kDa. There were  $1.4 \pm 0.4$  atoms of manganese present per subunit. The enzyme could be inhibited by  $\text{NH}_2\text{OH}$  but only weakly inhibited by cyanide or azide. The enzyme was colorless at concentrations of 0.7 mg/ml.

An apparently similar catalase has also been isolated from the bacterium *T. thermophilus* (163). The enzyme is approximately 210 kDa; each subunit is 34 kDa, indicating the existence of six subunits. The visible spectrum of the enzyme has a maximum near 440 nm ( $\epsilon = 7.7 \times 10^2 \text{ M}^{-1} \text{ cm}^{-1}$ ) with shoulders at 460 and 500 nm. The similarity of the visible spectrum when compared to that of the pseudocatalase of *L. plantarum* led the authors to speculate that this might be a Mn pseudocatalase; however, no metal analyses were reported. Additionally, the enzyme was inhibited by hydroxylamine, but it was also sensitive to azide.

Subsequent studies using low-temperature EPR measurements indicated that the active site of this enzyme was composed of a dinuclear manganese complex (165). In the temperature range 50–70 K, the EPR spectra of initial preparations revealed two superimposed signals: a 22-line component and a 16-line component. The structure of this protein has also been determined by X-ray crystallography to a resolution of 3 Å (166). The enzyme is composed of six subunits. Each subunit has four large  $\alpha$  helices disposed such that they run essentially parallel to each other. The dinuclear metal center rests in the middle, between the helices. The two Mn atoms have a separation of  $\sim 3.6$  Å. Interestingly, each subunit of the Fe-binding protein hemerythrin is also composed of four parallel  $\alpha$  helices with the binuclear active site positioned in the center of the helices [(167) and vide infra].

## B. MODEL STUDIES

The possibility that Mn catalase possesses a dinuclear center raises the question of whether any synthetic dinuclear complexes can mimic the spectroscopic properties and reactivity of the biological site. A number of dinuclear complexes containing Mn(II), Mn(III), and/or Mn(IV) have been characterized by X-ray diffraction techniques. These

TABLE VII

STRUCTURAL PARAMETERS FOR SYNTHETIC DINUCLEAR COMPLEXES

Complex	Mn...Mn	Mn-O <sub>b</sub>	Mn-O-Mn	Reference
Mn(III) <sub>2</sub> O(OAc) <sub>2</sub> (HB(pz) <sub>3</sub> ) <sub>2</sub>	3.159	1.773, 1.787	125.1	(168)
Mn(III) <sub>2</sub> O(OAc) <sub>2</sub> (TACN) <sub>2</sub> <sup>2+</sup>	3.084	1.80	117.9	(169)
Mn <sub>2</sub> (III, IV)O(OAc) <sub>2</sub> (Me <sub>3</sub> TACN) <sub>2</sub> <sup>3+</sup>	3.230	1.826, 1.814	125.1	(170)
Mn <sub>2</sub> (III, IV)O <sub>2</sub> (OAc)(TACN) <sub>2</sub> <sup>2+</sup>	2.588	1.817, 1.808	91.1	(171)
Mn(III) <sub>2</sub> O(OAc) <sub>2</sub> Cl <sub>2</sub> (bipy) <sub>2</sub>	3.153	1.788, 1.777	124.3	(182)
Mn <sub>2</sub> (III, IV)O <sub>2</sub> (OAc)Cl <sub>2</sub> (bipy) <sub>2</sub>	2.667	1.827, 1.843, 1.805, 1.793	94.52, 94.35	(183)

complexes display a range of types of bridging ligands such as thiolate (Section III,B), imidazolate (Sections II,B and III,B), carboxylate (132, 168–171), phenoxide or alkoxide (Section IV,B), oxide (168–176), and hydroxide (131).

A similarity in the visible spectra of some  $\mu$ -oxo-di- $\mu$ -acetato Mn(III) dinuclear complexes to the spectrum of Mn catalase has been noted (168–174). Reaction of hydrotris(1-pyrazolyl)borate, [HB(pz)<sub>3</sub>]<sup>−</sup>, or 1,4,7-triazacyclononane (TACN) with “Mn(OAc)<sub>3</sub>·2H<sub>2</sub>O” results in the formation of the dinuclear complexes [Mn<sub>2</sub><sup>III</sup>O(OAc)<sub>2</sub>(HB(pz)<sub>3</sub>)<sub>2</sub>] (168) and [Mn<sub>2</sub><sup>III</sup>O(OAc)<sub>2</sub>(TACN)<sub>2</sub>]<sup>2+</sup> (169). Selected structural parameters are given in Table VII. The dimanganese cores of the complexes are essentially identical to those of some  $\mu$ -oxo-di- $\mu$ -carboxylato diiron(III) complexes (177, 178), which have been shown to be excellent structural models of the diiron site in methemerythrin (Fig. 8) (179).

The tris(pyrazolyl)borate Mn complex in acetonitrile displays a

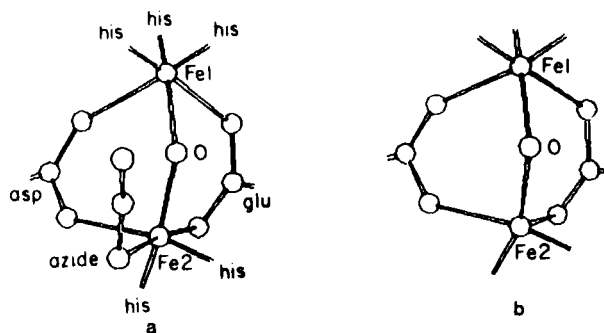


FIG. 8. The structures of the iron centers in azidomethemerythrin (A) and methemerythrin (B). (Reproduced from Ref. 179 with the authors' permission.)

quasireversible oxidation at 0.51 V (versus ferrocene) corresponding to the formation of the  $\text{Mn}_2(\text{III,IV})$  mixed-valence compound and a second quasireversible oxidation presumably to the  $\text{Mn}_2(\text{IV,IV})$  complex at +1.22 V (168). For the TACN complex, cyclic voltammograms of an acetonitrile solution exhibited a quasireversible oxidation to the mixed-valence dimanganese complex at 0.59 V (169). Using the ligand  $\text{Me}_3\text{-TACN}$ , this mixed-valence species has been generated chemically and characterized by X-ray techniques (Fig. 9) (170). In liquid  $\text{SO}_2$  ( $-40^\circ\text{C}$ ), the  $\text{Mn}_2(\text{III,IV})$  dimer could be reversibly converted to the  $\text{Mn}_2(\text{IV,IV})$  species (1.92 V versus NHE).

Magnetic susceptibility studies, however, reveal some significant differences between the complexes. The  $\text{HB}(\text{pz})_3$  complex exhibits antiferromagnetic coupling ( $H = -2JS_1 \cdot S_2$ ) with  $J \sim -0.5 \text{ cm}^{-1}$  (168); the TACN analog is ferromagnetically coupled with  $J = +18 \text{ cm}^{-1}$  (169). The mixed-valence complex exhibits somewhat more significant spin exchange with an antiferromagnetic coupling constant of  $J = -40 \text{ cm}^{-1}$  (170).

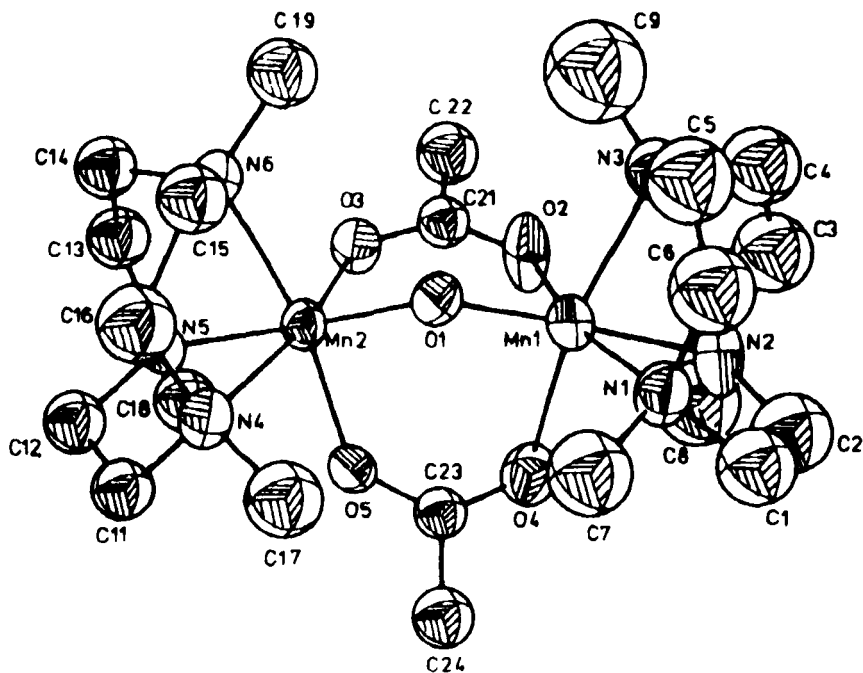


FIG. 9. The structure of  $[\text{Mn}_2\text{O}(\text{O}_2\text{CMe})_2(\text{Me}_3\text{-TACN})_2]^{3+}$ . (Reproduced with permission from Ref. 170. Copyright 1986, Verlag Chemie.)

TABLE VIII

 UV/VISIBLE DATA FOR Mn CATALASE AND  
 SYNTHETIC DINUCLEAR COMPLEXES

Species	$\lambda_{\max}$ (nm) <sup>a</sup>
Mn catalase	398, 470(135), 500
$\text{Mn}_2\text{O}(\text{OAc})_2(\text{TACN})_2^{2+}$	486(337), 521(323)
$\text{Mn}_2\text{O}(\text{OAc})_2(\text{HB}(\text{pz})_3)_2$	385(sh), 486(210), 503(sh), 760(58)
$\text{Mn}_2\text{O}(\text{OAc})_2\text{Cl}_2(\text{bipy})_2$	492(350), 556(246)

<sup>a</sup> Data in parentheses are  $\epsilon/\text{Mn}_2$ .

The TACN complex gave two visible absorptions at 486 and 521 nm ( $\epsilon/\text{Mn} = 337$  and  $323 \text{ M}^{-1} \text{ cm}^{-1}$ , respectively), while the visible spectrum of the oxidized complex is similar in shape (169, 170). The  $\text{HB}(\text{pz})_3$  complex has bands at 486 ( $\epsilon = 210 \text{ M}^{-1} \text{ cm}^{-1}$ ) and 760 nm ( $\epsilon = 58 \text{ M}^{-1} \text{ cm}^{-1}$ ) (168). For comparisons to the enzyme, see Table VIII.

Hydrolysis of  $\text{Mn}_2\text{O}(\text{OAc})_2(\text{Me}_3\text{TACN})_2^{2+}$  results in overall displacement of one of the bridging acetate ligands to give  $\text{Mn}_2(\text{III,IV})\text{-O}_2(\text{OAc})(\text{Me}_3\text{-TACN})_2^{2+}$  (Fig. 10) (171). The lost acetate is thus

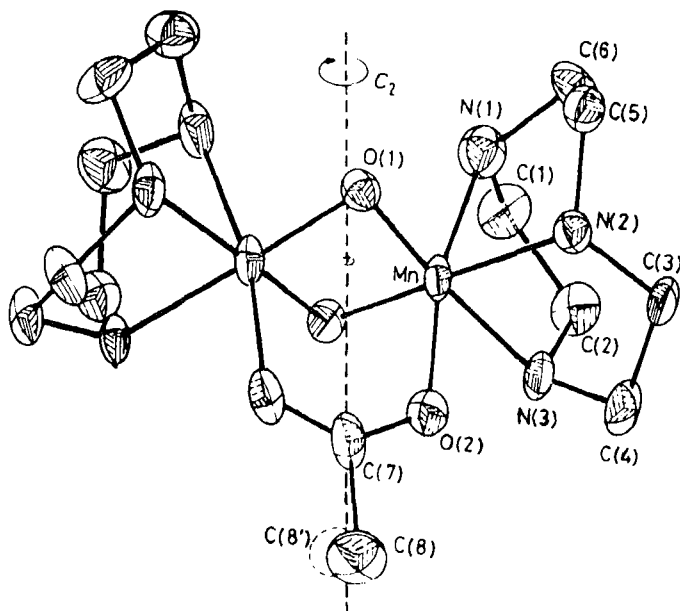


FIG. 10. The structure of  $[\text{Mn}_2\text{O}_2(\text{O}_2\text{CMe})(\text{TACN})_2]^{2+}$ ; the dashed line indicates an imposed twofold axis. (Reproduced with permission from Ref. 171. Copyright 1987, Royal Society of Chemistry.)

replaced by a bridging oxide concomitantly with oxidation of one manganese. The antiferromagnetic coupling within the  $[\text{Mn}_2\text{O}_2(\text{OAc})]$  core ( $J = -220 \text{ cm}^{-1}$ ) is an order of magnitude greater than that in the dimers with a single oxide bridge; this probably indicates that the majority of spin coupling is propagated by the oxide bridges. The low-temperature EPR spectrum displayed 16 hyperfine lines centered at  $\sim g = 2.00$ . Reaction of aqueous permanganate with the  $\text{HB}(\text{pz})_3$  dimer results in the formation of a new complex characterized by EPR, Raman, and mass spectrometry to be the analogous di- $\mu$ -oxo- $\mu$ -acetato compound (168).

While the corresponding dinuclear Fe complexes with TACN and  $\text{HB}(\text{pz})_3$  are excellent structural models for the metal site in hemerythrin, their reactivity varies greatly from that of the natural system where dioxygen binds to a terminal site on one iron (179). Similarly, reaction of the synthetic  $\text{Mn}_2$  complexes with substrate analogs (such as  $\text{N}_3^-$  and  $\text{SCN}^-$ ) which bind to the  $\text{O}_2$ -binding site of the protein results in displacement of the bridging ligands (180, 181). This has spurred the synthesis of these types of dinuclear complexes without tridentate ligands, such that a binding site could be available for substrate analogs. Toward this end, Vincent *et al.* have synthesized and characterized the complex,  $\text{Mn}_2^{III}\text{O}(\text{OAc})_2\text{Cl}_2(\text{bipy})_2$  (Fig. 11

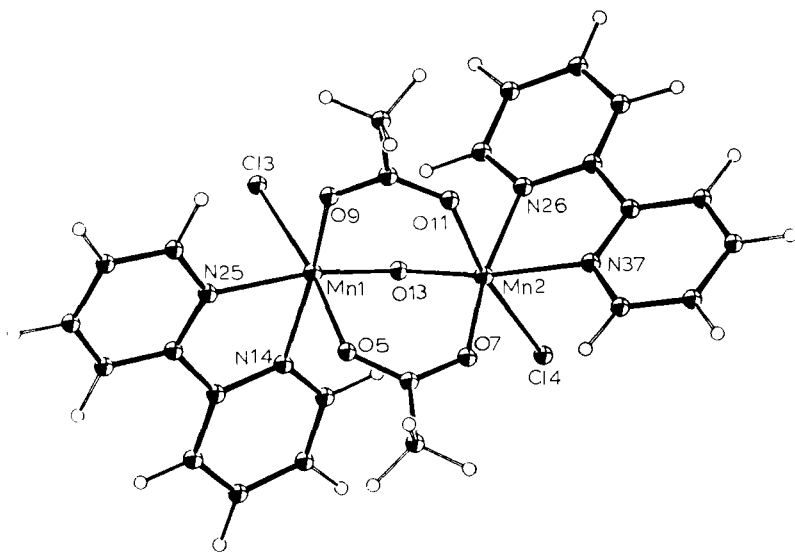


FIG. 11. The structure of  $\text{Mn}_2\text{O}(\text{O}_2\text{CMe})_2\text{Cl}_2(\text{bipy})_2$ .

and Table VIII) (182). In this complex, the tridentate ligands have been replaced by a bidentate bipyridyl and a chloride. When benzoic acid is utilized in place of acetate, substitution of the chlorides has been accomplished using  $\text{NaN}_3$  to give the structurally characterized complex,  $\text{Mn}_2\text{O}(\text{O}_2\text{CPh})_2(\text{bipy})_2(\text{N}_3)_2$ . The binding of azide suggests that peroxide might also bind in a similar manner to the synthetic complex as it does in oxyhemerythrin. Indeed, the  $\text{Mn}_2$  complex with Cl ligation has been shown to decompose a 100-fold excess of  $\text{H}_2\text{O}_2$ . The corresponding di- $\mu$ -oxo- $\mu$ -acetate complex  $\text{Mn}_2\text{O}_2(\text{OAc})(\text{bipy})\text{Cl}_2$  has been synthesized from the reaction of  $\text{Me}_3\text{SiCl}$  and bipy with " $\text{Mn}(\text{OAc})_3 \cdot 2\text{H}_2\text{O}$ " and has been structurally characterized (183) (see Table IX).

In summary, the variety of oxidation levels readily obtainable by these  $\mu$ -oxide- $\mu$ -carboxylate complexes and their reactivity with dioxygen analogs suggest that they may well prove to possess a high degree of structural correspondence to the  $\text{Mn}_2$  site within the catalase enzyme. This belief is supported by the tertiary structural similarity between catalase and hemerythrin, and the similar structure of the  $\text{Fe}_2\text{O}(\mu\text{-O}_2\text{CR})_2$  unit in the latter protein and its synthetic models.

TABLE IX  
STRUCTURAL PARAMETERS FOR OXIDE-BRIDGED DINUCLEAR COMPLEXES

Complex	Mn-O <sub>b</sub> (Å)	Mn...Mn (Å)	Reference
Linear oxide bridge			
$\text{Mn}(\text{IV})_2\text{O}(\text{TPP})_2^{2+}$	1.743(4), 1.794(4)	3.537(4)	(299)
$\text{Mn}(\text{III})_2\text{O}(\text{phthal})_2$	1.71(1)	3.42(1)	(175)
$\text{Mn}(\text{III})_2\text{O}(\text{CN})_{10}^{6-}$	1.723(4)	3.446(4)	(176)
Bent oxide bridge			
$\text{Mn}_2(\text{III,III})\text{O}(\text{OAc})_2(\text{HB}(\text{pz})_3)_2$	1.773(2), 1.787(2)	3.159(1)	(168)
$\text{Mn}_2(\text{III,III})\text{O}(\text{OAc})_2(\text{TACN})_2^{2+}$	1.80(1)	3.084(3)	(167)
$\text{Mn}_2(\text{III,IV})\text{O}(\text{OAc})_2(\text{Me}_3\text{TACN})_2^{3+}$	1.826(6), 1.814(6)	3.230(3)	(170)
$\text{Mn}_2(\text{III,III})\text{O}(\text{OAc})_2\text{Cl}_2(\text{bipy})_2$	1.788(11), 1.777(12)	3.153(1)	(182)
Di- $\mu$ -oxide bridge			
$\text{Mn}_2(\text{III,IV})\text{O}_2(\text{bipy})_2^{3+}$	1.784–1.856	2.716(2)	(172)
$\text{Mn}_2(\text{III,IV})\text{O}_2(\text{phen})_2^{3+}$	1.808(3), 1.820(3)	2.700(1)	(174)
$\text{Mn}_2(\text{IV,IV})\text{O}_2(\text{phen})_2^{4+}$	1.797–1.805	2.748(2)	(174)
$\text{Mn}_2(\text{III,IV})\text{O}_2(\text{OAc})(\text{TACN})_2^{2+}$	1.817(5), 1.808(4)	2.588(2)	(171)
$\text{Mn}_2(\text{III,IV})\text{O}_2(\text{OAc})(\text{bipy})_2\text{Cl}_2$	1.793–1.843	2.667(2)	(183)
Di- $\mu$ -hydroxo bridge			
$\text{Mn}(\text{III})_2(\text{OH})_2(\text{salpn})_2$	Not reported	2.72	(131)



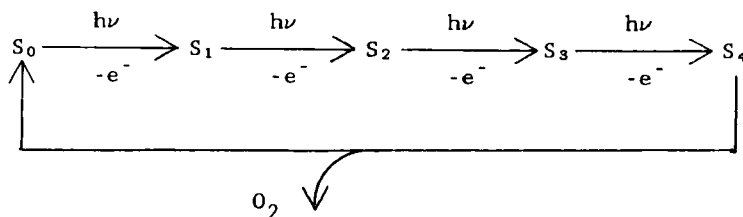
## VI. Photosystem II

## A. THE NATIVE SYSTEM

## 1. Introduction

By far the most important role of manganese in nature is its direct involvement in the photocatalytic, four-electron oxidation of water to dioxygen in green plant photosynthesis, an essential process for the maintenance of life. Pirson, in 1937, first discovered the requirement of manganese in photosynthesis by showing that plants grown in a Mn-deficient medium lost their water oxidation capacity (184). During the next four decades, several researchers showed that two photosystems, photosystem I (PSI) and photosystem II (PSII), were involved in photosynthesis and that  $O_2$  evolution and Mn were localized at PSII (for a review, see Ref. 185).

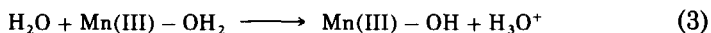
In a classical flash study, Kok *et al.* showed that the  $O_2$ -evolving complex of photosystem II is oxidized sequentially in a four-quantum, four one-electron oxidative process, the steps being named  $S_0$ – $S_4$ , with  $S_0$  representing the totally reduced form (186). In the  $S$  state model (Scheme 1),  $S_4$  is only transiently stable, rapidly converting to  $S_0$  with concomitant  $O_2$  evolution.



SCHEME 1.

In the dark, the  $S_2$  and  $S_3$  levels revert back to  $S_1$  to give a mixture, 75%  $S_1$  and 25%  $S_0$ . During prolonged dark adaption, the  $S_0$  level becomes oxidized to the  $S_1$  level (236). Thus, for dark-adapted systems, maximal oxygen evolution is seen after three flashes of light, which advance the  $S_1$  level to the  $S_4$  level. Mn, therefore, with its large number of readily accessible oxidation states is probably central to the stabilization of these oxidizing equivalents. Manganese in the photosynthetic apparatus is believed to function in three main ways: by acting as a template to hold two molecules of water in close proximity,

making oxygen–oxygen bond formation as facile as possible, by stabilizing oxidizing equivalents as described above, and by making the bound water more acidic so that  $H^+$  loss is more facile; Wells has shown that the equilibrium constant for the reaction given by Eq. (3) is at least two orders of magnitude larger for Mn(III) than any other first-row transition metal in the trivalent state (187). In spite of efforts to elucidate the structure of the Mn center operating in the photosynthetic enzyme of green plants and cyanobacteria, little is known about the arrangement of the metals, their ligation, or even the protein(s) with which the metal is associated.



Advances in the study of photosynthetic manganese and the water oxidation complex have been accelerated by the development of techniques for the isolation of “photosystem II particles” by Triton-X and/or digitonin treatment of thylakoid membranes (188, 189). Freeze-fracture electron microscopy indicates the particles are highly purified membrane fragments almost entirely devoid of photosystem I components (190). The lumenal side of the photosystem II membrane is exposed, allowing direct access to the water oxidation enzyme complex. These PSII preparations contain four atoms of manganese per PSII reaction center and possess large amounts of  $O_2$  activity (191, 192).

Recent work has resulted in the isolation of discrete PSII chlorophyll–protein aggregates which, to date, are the minimal units capable of oxygen evolution (193–195). These aggregates contain only one extrinsic protein (33 kDa) and a handful of intrinsic membrane proteins (47, 43, 32, and 30 kDa and two copies of cytochrome  $b_{559}$ ), while retaining approximately four Mn atoms. The molecular weights of these aggregates range from about 300 to 450 kDa.

The extrinsic 33-kDa protein, first isolated by Kuwabara and Murata (196), has been associated with Mn and with  $O_2$ -activity in both PSII particles and the PSII aggregates. This polypeptide has been isolated with bound Mn (197–199). Abramowicz and Dismukes observed that, when isolated in the presence of oxidants, the 33-kDa protein could bind a maximum of two Mn atoms per protein (197). Below 12 K, the protein exhibited an EPR signal centered at  $g = 2$  and extending over at least 2000 G. The signal was assigned to either an antiferromagnetically coupled  $Mn_2(II,III)$  site or a ferromagnetically coupled  $Mn_2(III,III)$  site, with the latter being preferred. Treatment of the Mn-containing protein with hydroxylamine or other reducing agents abolished the low-temperature EPR signal and released two Mn(II) ions into solution.

Amino acid analysis (196) and a complete amino acid sequence of the 33-kDa protein from spinach (201) indicated that no histidine was present. Thus, Mn ligation to this polypeptide must be to tyrosine phenoxide and/or to the carboxylate functionalities of aspartate and glutamate.

Removal of the 33-kDa protein by salt or urea washing of PSII particles or PSII complexes results in substantial loss of  $O_2$ -evolving activity but retention of Mn (202–204). However, with time, two of the four Mn are lost (202, 203). Rebinding of the 33-kDa protein restored  $O_2$  activity (204, 205); hence, the polypeptide is believed to stabilize Mn binding, presumably through direct interaction with the metal. Quantitative analysis of the rebinding suggests a specific binding site for the polypeptide on the membrane (209) and the presence of Mn enhances rebinding (205). Koike and Inoue have shown that binding of an extrinsic 34-kDa protein from a cyanobacterium partially reconstitutes spinach PSII particles lacking the 33-kDa polypeptide and that the spinach protein reactivated the depleted cyanobacterial system (210). The effect of removing the 33-kDa protein has been shown to be the prevention specifically of the  $S_3$  to ( $S_4$  to)  $S_0$  transition (206–208). The lack of the protein also appears to stabilize the  $S_1$  and  $S_2$  levels (206, 220). Consequently, this polypeptide is believed to hold the dioxygen-evolving apparatus in a conformation which stabilizes the transient species formed at the  $S_4$  level (207, 220).

Bowly and Frasch modified the 33-kDa protein with a photoaffinity label and rebound the protein to photosystem II preparations (200). Illumination then cross-linked the polypeptide to other polypeptides within 10 Å to give a protein complex. This complex contained three to four Mn atoms and consisted of proteins corresponding to molecular weights of 22, 24, 26, 28, 29, and 31 kDa. The 26-, 28-, and 29-kDa polypeptides are probably associated with the light-harvesting complex of PSII. The 22- and 24-kDa proteins had previously been shown to be associated with the 33-kDa protein by immunological studies (211), but this complex did not retain Mn. Rebinding studies have also implicated an association between the 24-kDa protein and the 33-kDa polypeptide (212). Only the 31-kDa protein is probably a component of oxygen-evolving PSII complexes, being one of the approximately 30-kDa intrinsic polypeptides. The intrinsic 43-kDa component of PSII complexes has also been proposed to be associated with the 33-kDa protein, based on protease treatment of PSII particles (213); however, this interpretation has recently been questioned (214). Recent immunochemical studies have also indicated that the 43- and 33-kDa polypeptides may be adjacent (223).

The intrinsic 32-kDa protein, or herbicide-binding protein, has also been implicated in Mn binding (215, 216). PSII preparations from the green alga *Scenedesmus obliquus* and its LF-1 mutant are nearly identical except that the mutant preparation is blocked on the oxidizing side of PSII and has a reduced Mn content (215). The difference seems to be related to a 34-kDa protein in the wild type which is not present in the mutant but is replaced by a 36-kDa protein, the only observable protein alteration (216). Herbicide-binding experiments (217) and immunological studies (218) indicate conclusively that this 34-kDa protein corresponds to the intrinsic herbicide-binding protein, the best characterized of all PSII complex components (for a review, see Ref. 219).

Iodolabeling studies on photosystem II particles from higher plants and cyanobacteria (221) and on a PSII complex (227) specifically labeled the herbicide-binding protein. As  $I^-$  is believed to donate electrons to Z, the secondary electron donor which is believed to accept electrons from the photosynthetic manganese complex, these experiments indicate a role for this protein on the oxidizing side of PSII. Consequently, Z must at least be located near, if not in, the herbicide-binding polypeptide (222).

The nucleotide sequence of the gene which encodes for the 32-kDa herbicide-binding protein has been sequenced from a variety of plant and algal sources (219). The sequence shows a high degree of homology to that of the intrinsic 34-kDa protein, whose gene has also recently been sequenced (224). Both of these proteins, in turn, show several regions which are homologous to portions of the L and M subunits of the photosynthetic reaction center of purple bacteria (225). The structure of the reaction center from the purple bacterium *Rhodospseudomonas viridis* has been determined at 3-Å resolution by X-ray crystallographic analysis (226), revealing the positions of the pigments and quinones involved in charge separation and electron transport. The regions of strong homology between the purple bacterium proteins and the PSII polypeptides correspond to the residues involved in pigment and quinone binding; this led to the proposal that the 32- and 34-kDa proteins form the PSII reaction center (225, 226). [Additionally, protease and antisera treatment of the two PSII membrane proteins have shown that the folding of the polypeptides were nearly identical to those of the L and M subunits (227, 228).] The hypothesis was confirmed when Nanba and Satoh isolated a three-protein complex consisting of the 32- and 34-kDa protein and a copy of cytochrome  $b_{559}$ , which possessed the pigments responsible for charge separation (229–231). Antisera experiments have also revealed that removal of the 33-kDa extrinsic protein and associated extrinsic polypeptides exposed an area

of the 32-kDa protein (228); thus, these extrinsic polypeptides must be in close association with the herbicide-binding protein.

All this evidence seems to indicate the tetranuclear complex involved in photosynthetic water oxidation spans a region between the intrinsic 32-kDa protein and the extrinsic 33-kDa polypeptide, which may explain the difficulties in isolating the intact complex. Ligation to the manganese would then be through tyrosine, glutamate, and/or aspartate residues of the extrinsic protein and these residues and possibly histidine residues of the intrinsic protein. The region of the 32-kDa protein implicated as a possible Mn-binding site mentioned above is quite rich in carboxylate functionalities. Ligation other than by amino acid side-chain moieties appears unlikely; no porphyrins have been found associated with the manganese. Despite the synthesis of a number of synthetic manganese catecholates (232, 233) and the importance of quinones in electron transport in the photosynthetic apparatus, such manganese complexes cannot comprise the photosynthetic metal assembly, as all quinones associated with the photosystem II reaction center have been accounted for in other functions (234). A highly oxidized Mn site seems unlikely to be supported by a flavin-derived molecule, as has been recently suggested (235).

## 2. Difference Ultraviolet/Visible Spectroscopy

Detailed absorbance difference spectra of PSII particles were first reported by Dekker *et al.* in 1984 (237). After corrections for contributions from donor and acceptor species, the difference spectra for the  $S_1$ -to- $S_2$  transition consisted of a broad, asymmetric band with a maximum at approximately 305 nm. The band was assigned to the oxidation of the donor involved in oxygen evolution. Comparison of these spectra with the difference spectra of a series of binuclear Mn-gluconate complexes described by Bodini *et al.* (243), which contain Mn in the divalent, trivalent, and tetravalent states, was carried out. The shape of the  $S_1$ -to- $S_2$  transition spectra more closely resembled the Mn(III)  $\rightarrow$  Mn(IV) change of the models; consequently, the absorbance at  $\sim 305$  nm was assigned to a Mn(III)  $\rightarrow$  Mn(IV) oxidation. The spectra also displayed a shoulder at 350 nm which the authors believed was significant. Further studies using a series of saturating flashes on dark-adapted submembrane fragments indicated that the  $S_0 \rightarrow S_1$ ,  $S_1 \rightarrow S_2$ , and  $S_2 \rightarrow S_3$  transitions were all accompanied by the same absorbance spectra with the maximum at  $\sim 305$  nm (238). Correspondingly, a negative absorbance with the same shape but of three times the magnitude of the others was found for the  $S_3 \rightarrow (S_4) \rightarrow S_0$

transition, reflecting a reduction by three units. The +1, +1, +1, -3, sequence of Mn oxidations during the  $S_0 \rightarrow S_1$ ,  $S_1 \rightarrow S_2$ ,  $S_2 \rightarrow S_3$ , and  $S_3 \rightarrow S_0$  transitions was later confirmed by measuring the kinetics of the flash-induced absorption changes (239); the half-lives found for these transitions, 30, 110, 350, and 1300  $\mu\text{sec}$ , respectively, are in excellent agreement with those measured by other techniques (247, 248).

However, Lavergne (240) and Renger and Weiss (241) presented alternative interpretations of the difference spectral data. To differentiate between the various proposals, Saygin and Witt (242) measured the absorbance difference spectra in the presence and absence of low concentrations of hydroxylamine, which shifts the  $S$  states by reduction backward two units. These experiments confirmed the +1, +1, +1, -3 redox change pattern.

The presence of a  $\text{Mn(III)} \rightarrow \text{Mn(IV)}$  transition during the first three  $S$ -state advances is hard to reconcile with results of XANES and EPR studies of the photosynthetic Mn (Sections VI,A,3 and VI,A,4). The choice of the Mn-gluconates as a model system stemmed from the distinct lack of isostructural Mn complexes in various oxidation levels; this polyalkoxide ligand is quite a departure from the ligand types believed to occur in the enzyme. Even in the case of the gluconates, the structure was inferred by a combination of electrochemistry and UV/vis spectroscopy and was not confirmed by X-ray crystallography (243). Recent work has shown that the difference ultraviolet spectra between isostructural  $\text{Mn}_3^{\text{III}}\text{O}(\text{OAc})_6(\text{py})_3^+$  and  $\text{Mn}_3^{\text{II,III,III}}\text{O}(\text{OAc})_6(\text{py})_3$  are strikingly similar to that reported by Dekker *et al.* (Fig. 12); thus, the enzyme spectra *could* result from a  $\text{Mn(II)} \rightarrow \text{Mn(III)}$  transition (244). Shortly thereafter, Witt *et al.* extracted the difference spectra of each individual  $S$ -state transition in the presence of  $\text{NH}_2\text{OH}$ , which should give purer  $S$  states on illumination (245). The absorption spectra resulting from the  $S_0 \rightarrow S_1$  transition possessed a maximum at 305–310 nm and was assigned to a  $\text{Mn(II)} \rightarrow \text{Mn(III)}$  oxidation, while the  $S_1 \rightarrow S_2$  and  $S_2 \rightarrow S_3$  transitions resulted in identical spectra with maxima shifted to  $\sim 340$  nm (Fig. 13). This shift to lower energy is that expected for a  $\text{Mn(III)} \rightarrow \text{Mn(IV)}$  transition. Interestingly, the original spectra of Dekker *et al.* are quite consistent for a mixture of the  $\sim 305$ - and  $\sim 340$ -nm spectra. Together, the above results suggest the following Mn oxidation state changes to be involved during the  $S$ -state transitions:  $S_0 \rightarrow S_1$ ,  $\text{Mn}^{\text{II}} \rightarrow \text{Mn}^{\text{III}}$ ;  $S_1 \rightarrow S_2$  and  $S_2 \rightarrow S_3$ ,  $\text{Mn}^{\text{III}} \rightarrow \text{Mn}^{\text{IV}}$ .

Another absorption attributed to the photosynthetic manganese center has been identified recently in the near infrared ( $\lambda_{\text{max}} \sim 780$  nm,  $\epsilon \cong 500 \text{ M}^{-1} \text{ cm}^{-1}$ ) (246). Treatment of PSII particles which release manganese abolish this signal. The absorbance oscillates in intensity with flashes and is maximal in the  $S_2$  and  $S_3$  levels. The energy and

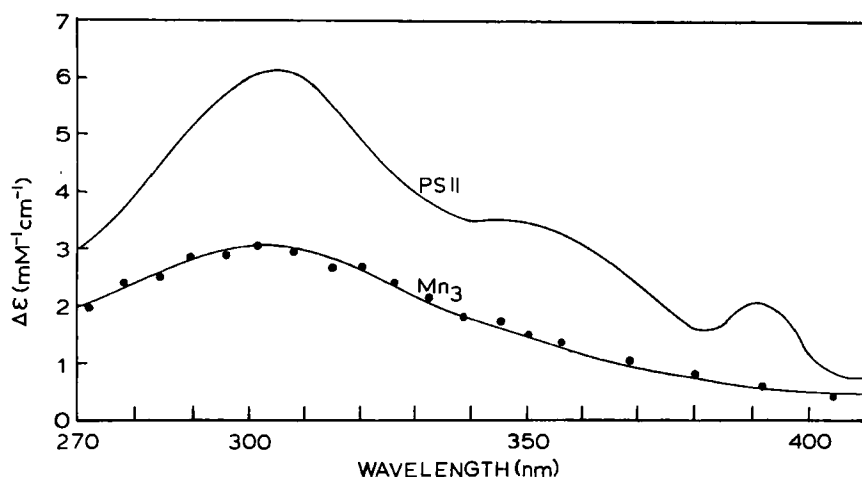


FIG. 12. Difference absorbance spectra for  $[\text{Mn}_3\text{O}(\text{O}_2\text{CMe})_6(\text{pyr})_3]^{0+}$  and the enzyme site, labeled  $\text{Mn}_3$  and PSII, respectively. (Reproduced with permission from Ref. 244. Copyright 1986, Federation of European Biochemical Societies.)

intensity of this band are similar to the band resulting from the intervalence  $\text{Mn(III)} \rightarrow \text{Mn(IV)}$  transition in  $[\text{Mn}_2\text{O}_2(\text{bipy})_4]^{3+}$  (249) and have been attributed as such to an intervalence band in the enzyme. However, the presence of an intervalence band at  $\sim 700\text{--}800\text{ nm}$  is not a

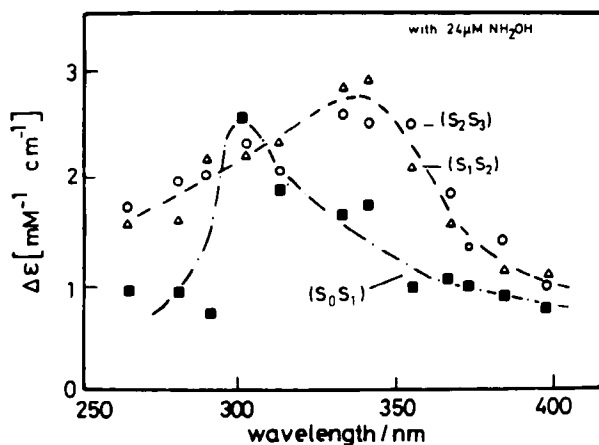


FIG. 13. Difference absorbance spectra for PSII at different  $S$ -state transitions in the presence of  $\text{NH}_2\text{OH}$ . (Reproduced with permission from Ref. 245. Copyright 1986, Martinus Nijhoff Publishers.)

general property of trapped-valence Mn(III,IV) dimers (170, 171), and this assignment must be considered tentative.

### 3. EXAFS and Edge Studies

Recent EXAFS results have provided the most detailed information on the coordination sphere of the Mn. Studies on PSII particles posed in the  $S_1$  level disclose that at least two metals occur as a dinuclear species with a  $\text{Mn} \cdots \text{Mn}$  separation of approximately 2.7 Å (250). Low-atomic-weight atoms, N or O, are found at distances of  $\sim 1.75$  and  $\sim 1.98$  Å, and are characteristic of bridging oxide (or presumably hydroxide) ligands and terminal ligands, respectively.

Best-fit parameters determined are given in Table X. These data would seem to preclude  $\text{Cl}^-$  binding or sulfur-based ligation. These studies are thus consistent with manganese ligation composed solely of the amino acid side-chain functions of histidine, tyrosine, glutamic and/or aspartic acid, and the forms of oxygen in its various oxidation levels (i.e.,  $\text{O}_2$ ,  $\text{O}_2^-$ ,  $\text{O}_2^{2-}$ ,  $\text{O}^{2-}$ ,  $\text{OH}^-$ , and  $\text{H}_2\text{O}$ ). The EXAFS data are also consistent with the presence of additional manganese atoms greater than 3.0 Å from the dinuclear center. The  $k^3$ -weighted EXAFS data preferentially enhanced the peak assigned to the manganese atom at  $\sim 2.69$  Å, confirming its assignment. Additionally, a preedge feature assigned as a  $1s \rightarrow 3d$  transition indicates most of the Mn is in a specialized noncentrosymmetric environment.

Illumination of the PSII particles at 190 K results in formation of the  $S_2$  level and causes a shift in the Mn K-edge spectra from 6551.3 to 6552.5 eV, indicative of oxidation of manganese during the  $S_1$  to  $S_2$

TABLE X  
INTERATOMIC SEPARATIONS<sup>a</sup> IN MODEL COMPLEXES AND THE NATIVE SITE

	$\text{Mn}_4\text{O}_2^-$ (OAc) <sub>7</sub> (bipy) <sub>2</sub> <sup>+</sup>	$\text{Mn}_4\text{O}_2^-$ (OAc) <sub>6</sub> (bipy) <sub>2</sub>	$\text{Mn}_4\text{O}_3\text{Cl}_6^-$ (HIm)(OAc) <sub>3</sub> <sup>2-</sup>	PSII EXAFS
Mn $\cdots$ Mn (short)	2.848(0.5)	2.779(0.5)	2.814(1.5)	2.69 <sup>b</sup> (0.68)
Mn $\cdots$ Mn (long)	3.342(2.0)	3.385(2.0)	3.285(3)	$\sim 3.3$ (not reported)
Mn-oxide	1.882(1.5)	1.854(1.0) <sup>c</sup>	1.920(2.3)	1.75(3)(2.27) <sup>d</sup>
Mn-N,O	2.073(4.5)	2.138(4.5)	2.057(1.75)	2.05(3)(3.25) <sup>d</sup>

<sup>a</sup> Average distances (Å); numbers in parentheses indicate number of atoms at this distance.

<sup>b</sup> The e.s.d. is  $\pm 0.03$  Å.

<sup>c</sup> Mn(III)-oxide.

<sup>d</sup> Value  $\pm 20\%$ .



transition (251). The preedge feature at  $\sim 6543$  eV is retained. EXAFS of the  $S_2$  level show that the important features are essentially identical for samples in the  $S_1$  and  $S_2$  states. Therefore, no significant change in the coordination of manganese occurs during the  $S_1$ -to- $S_2$  transition. Again, no evidence for  $\text{Cl}^-$  binding could be found. Similar studies on photosystem II particles from the cyanobacterium *Synechococcus* reveal similar edge shapes, including the preedge feature; a shift in edge inflection points from 6551.1 to 6552.1 eV during the advancement from  $S_1$  to  $S_2$ ; Mn, O, and N atoms at similar distances; and a lack of chloride or sulfur ligands (252). Analyses on the sum of EXAFS spectra of PSII particles have indicated a fourth scattering shell (253). This shell, which is enhanced by  $k^3$  weighting, has been assigned to additional manganese at 3.3 Å from the dinuclear manganese site, evidence for a tetranuclear manganese complex.

The EXAFS and Mn- $K$  edge spectra of PSII particles partially advanced to the  $S_3$  level ( $\sim 47\%$ ) by illumination at 235 K have also been examined (253). The edge inflection point occurred at 6552.4 eV, identical to that of  $S_2$  (within experimental error). This may indicate that no oxidation state change of the tetranuclear manganese complex has occurred during the  $S_2$  to  $S_3$  transition. EXAFS data on this advanced  $S$  level are consistent with retention of the short Mn $\cdots$ Mn separation and of the terminal and bridging oxygen- and nitrogen-based ligands.

Treatment of PSII particles posed in the  $S_1$  level with  $\text{NH}_2\text{OH}$  results in no appreciable shift of the inflection point of the Mn- $K$  edge; thus, no reduction of manganese occurs in the dark in the presence of this reagent (253). When the particles are illuminated, the inflection point shifts to lower energy, 6550.2 eV, corresponding to the generation of an " $S_0$ " level (which may or may not be equivalent to the naturally occurring  $S_0$  level). The magnitude of this shift is very similar to that of the  $S_1$ -to- $S_2$  advancement and, therefore, is believed to indicate reduction of a manganese center(s). Combined with simultaneous EPR studies, these results provided evidence that a two-electron reduction of the tetranuclear manganese complex occurs concurrent with the  $S_1$ -to- $S_2$  transition in the presence of  $\text{NH}_2\text{OH}$ . EXAFS studies of the " $S_0$ " level indicated some differences from the higher  $S$  levels. The short Mn $\cdots$ Mn separation had increased to about 2.8 Å, and some terminal N or O ligands appeared to occur at distances up to  $\sim 2.2$  Å. The changes in the  $K$  edge and EXAFS on illumination indicate that the water analog,  $\text{NH}_2\text{OH}$ , binds near to the manganese, presumably concurrent with the advancement of the  $S_1$  level to the  $S_2$  level.

EXAFS and XANES studies have also been performed on  $\text{CaCl}_2$ -washed PSII particles (251). Edge spectra and EXAFS results of samples still retaining four manganese (but lacking the extrinsic 33-kDa protein) were similar to those of untreated particles in the  $S_1$  level. The edge inflection of samples containing only two Mn was shifted to 6548.9 eV, suggesting the metal ions were in the divalent oxidation state ( $\text{Mn}^{2+}$  aqueous, 6548.5 eV) (254); EXAFS results indicated that the two metal atoms were separated by a distance of over 4 Å. Apparently the basic structure of the tetranuclear Mn complex is retained upon loss of the 33-kDa extrinsic protein (under appropriate conditions).

#### 4. EPR and NMR

In 1980, Dismukes and Siderer first reported that electron spin resonance studies of spinach chloroplasts given a series of laser flashes and cooled rapidly to  $-140^\circ\text{C}$  revealed a signal centered at  $g = 1.96$  possessing at least 16 hyperfine lines when observed below 35 K (255). The  $g$  value was weakly anisotropic, and the average hyperfine separation of lines was 75–90 G. Additional hyperfine transitions in the wings of the spectrum outside of the prominent 16 inner lines appeared to be present. The intensity of the signal was maximal after one or five light flashes (256), corresponding to the  $S_2$  level of Kok's scheme. The line pattern of the EPR signal was shown based on simulations to be consistent with a pair of antiferromagnetically coupled manganese ions. Agents which reduced the amount of bound manganese abolished the signal. Further, the change in intensity of the signal with the laser flashes was concluded to indicate that oxidation state changes of the bound Mn were involved in the oxidation of water. For the remainder of this work, this signal shall be referred to as the multiline EPR signal.

Further simulations assuming a tetranuclear manganese complex of  $C_{2v}$  symmetry gave reasonable fits of the line pattern, including the wings, if three Mn(III) and one Mn(IV) were utilized (257). The simulations also indicated that the manganese atoms were deeply trapped valent and may be involved in both ferromagnetic and antiferromagnetic interactions. Brudvig and co-workers have shown that distinctly different  $S_2$  multiline signals can be detected for PSII particles dark adapted for varying periods of time and illuminated at temperatures between 130 and 273 K (262). These EPR signals are believed to arise from two states of the photosynthetic assembly: an active state resulting from short-term dark adaption and a resting state found in long-term adapted PSII particles.

Another EPR signal centered at  $g \sim 2$ , with very complex features

and extending over at least 4000 G, has been observed in dark-adapted whole cells of blue-green algae, green algae, and dark-adapted spinach thylakoid membranes below 8 K (258). The features of the spectrum are similar to those that would be expected from an even-spin ( $S > 0$ ) dinuclear or tetranuclear Mn complex.

Additionally, Casey and Sauer have found that illumination of dark-adapted photosystem II particles at 140 K produced, when cooled to 10 K, a 320 G-wide EPR signal centered near  $g = 4.1$  (259). Further studies showed that the production of the  $g = 4.1$  signal occurred concurrently with a shift in the Mn-K-edge inflection point in X-ray absorption spectra to higher energy (260); the shift was similar to that observed previously upon formation of the  $S_2$  multiline signal, indicative of advance from the  $S_1$  to  $S_2$  level. Consequently, the  $g = 4.1$  signal has been assigned to the Mn complex in the  $S_2$  level. Thus, two EPR signals appear to arise from the Mn assembly in the  $S_2$  level. Zimmerman and Rutherford have demonstrated from the oscillation pattern of the  $g = 4.1$  signal with light flashes that the signal corresponds to the  $S_2$  level (263). They also were able to generate both this signal and the multiline signal simultaneously, indicating both signals arise from different populations of the Mn centers. The authors believed that two Mn sites were present which differed slightly in structure, each giving rise to a different signal and that the  $g = 4.1$  signal arose from an  $S = \frac{3}{2}$  spin state of the tetranuclear manganese complex. de Paula *et al.* showed that warming to 200 K PSII particles which give rise to the  $g = 4.1$  signal yielded the multiline signal on cooling (264). Thus, these researchers concluded that both EPR signals arise from the same site in the  $S_2$  level and that the differences reflect temperature-dependent changes in the structure of the manganese center. In a series of studies on the orientation dependence of EPR signals arising from PSII membranes, Rutherford showed that the center giving rise to the  $g = 4.1$  signal was magnetically anisotropic with a fixed geometry in the membrane (261). The component giving rise to the multiline signal was also oriented within the membrane and showed some magnetic anisotropic character which was most marked as shifts in the position of the low-field wings of the spectrum. Examples of the two EPR signals are shown in Fig. 14.

Simulations of the temperature dependence of the EPR signals are beginning to reveal valuable information about magnetic interactions within the photosynthetic manganese complex. Using the Hamiltonian  $H = -JS_1 \cdot S_2$  for a dinuclear system, Hansson *et al.* estimated an exchange value of  $J = -19 \pm 4 \text{ cm}^{-1}$  (265). Dismukes and Damoder, using a model where a Mn dimer (a) interacted with another manganese

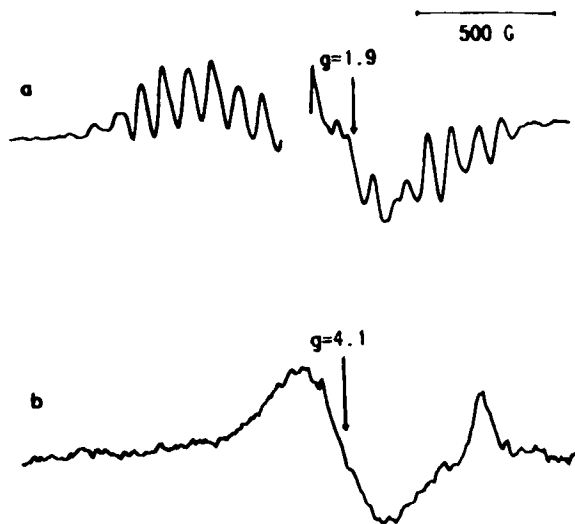


FIG. 14. EPR signals resulting from low-temperature illumination of PSII particles; (a)  $g = 2.00$  multiline signal, (b)  $g = 4.1$  signal. (Reproduced with permission from Ref. 268. Copyright 1986, American Chemical Society.)

site (b), obtained  $J = -17 \text{ cm}^{-1}$  and  $J_{ab} = -3 \text{ to } -4 \text{ cm}^{-1}$  (266). On cooling below 10 K, the multiline signal was shown to become maximal at approximately 6 K and to disappear on further cooling. Computer fits of the temperature dependence (267) indicated about four spin states were at lower energy than the  $S = \frac{1}{2}$  state which give rise to the multiline signal. Assuming an  $S = \frac{3}{2}$  ground state and an  $S = \frac{1}{2}$  first excited state for a tetranuclear manganese complex, de Paula *et al.* (268) determined that three exchange interactions were necessary to describe the temperature-dependent behavior of the multiline signal: a large antiferromagnetic exchange coupling between a  $\text{Mn}_2(\text{III,IV})$  pair ( $J$ ), a smaller antiferromagnetic coupling between a  $\text{Mn}(\text{III})_2$  pair ( $J'$ ), and the remaining interactions being ferromagnetic ( $J''$ ). The magnitude of the  $J$  values followed the pattern  $|J| \gg 3|J'| > |J''| > 2|J'|$ . Models with three trivalent manganese and a single divalent manganese, or with three tetravalent ions and a single trivalent manganese, gave equally good fits (268). However, Hansson *et al.* have shown from quantitation of the  $g = 4.1$  and the multiline signals between 5 and 23 K that the two signals arise from paramagnetic species in *different* PSII centers (269). They suggested that the two signals arise from species in a redox equilibrium and that the  $g = 4.1$  signal might arise from a mononuclear  $\text{Mn}(\text{IV})$  complex. Dismukes has also concluded

that there is no evidence that the two spectral forms arise simultaneously from the same manganese complex (270).

Perhaps the most valuable information obtained from EPR studies comes from ligand-binding studies. The  $S_2$  multiline signal produced in the presence of  $^{17}\text{OH}_2$  at 200 K possessed observable hyperfine broadening, indicating that oxygen ligands from water were bound to the manganese (271). Yachandra *et al.* have investigated the effect of different halides on the multiline signal (272). PSII particles and  $\text{Cl}^-$ -depleted particles which had been reconstituted with  $\text{Br}^-$  gave identical EPR signals, suggesting the halide ions were not ligands to the Mn center. Combined with EXAFS studies, the amount of  $\text{Cl}^-$  in the first coordination sphere of the Mn has been estimated to be less than 0.5  $\text{Cl}^-$  per 4 Mn (273). Velthuys, in flash-induced luminescence studies, has shown that  $\text{NH}_3$  does not bind to Mn in the  $S_1$  level but appears to bind in the  $S_2$  and  $S_3$  levels (274). The binding prevented advance to the  $S_4$  level. The binding of  $\text{NH}_3$  also appeared to decrease the redox potential of the  $S_2$  level. Recent EPR studies have verified Velthuys' results (275, 276). Generation of the multiline signal in the presence of  $\text{NH}_4\text{Cl}$  by illumination at  $0^\circ\text{C}$  prior to cooling results in change in the average hyperfine line spacing, indicating the presence of an interaction between ammonia and the manganese complex. Generation of the  $S_2$  state by illumination at 210 K in the presence of  $\text{NH}_4\text{Cl}$  did not yield the new signal, establishing that ammonia did not bind in the  $S_1$  level (276).

Spin echo studies of the multiline EPR signal have demonstrated that the photosynthetic Mn are accessible to exchangeable hydrogens of water (273, 277). No coupling of the manganese to  $^{14}\text{N}$  nuclei could be detected (277). For particles illuminated in the presence of ammonia, nitrogen modulation was exhibited, illustrating that ammonia was a ligand to the manganese complex in the  $S_2$  level (273). A broad signal centered at approximately  $g = 2$  with relaxation properties similar to the  $S_2$  signal but devoid of Mn hyperfine features has also been detected for the water-oxidizing complex in the  $S_1$  level (277). Spin-echo experiments measuring the relaxation time of the EPR signal arising from the oxidized form of D (an electron acceptor from the photosynthetic manganese complex very similar to Z but giving rise to a slower relaxing EPR signal) have shown that the spin-lattice relaxation times are dependent on the redox state of the manganese assembly (278). In advancing from the  $S_0$  level to the  $S_3$  level, the relaxation time decreased, consistent with an oxidation of manganese during each S-state transition. Additional EPR studies by Styring and Rutherford indicate that  $\text{D}^+$  can slowly oxidize the  $S_0$  level to the  $S_1$  level (279).

The authors propose that this is the mechanism by which the  $S_0$  level is slowly oxidized to  $S_1$  in the dark; this may be necessary to oxidize a  $Mn^{2+}$  ion in the  $S_0$  level to  $Mn^{3+}$  to prevent dissociation of a tetranuclear assembly and would, therefore, be similar to the photoactivation by which  $Mn^{2+}$  is incorporated into the enzyme (279, 283).

Alkaline salt washing of PSII particles reduces the intensity of the multiline signal in direct parallel with the loss of the extrinsic 33-kDa protein (and  $O_2$  evolution) (280). Between pH 8.0 and 9.5, this treatment was also found to release the four manganese ions with the first two to three manganese being released cooperatively. These results suggest that the 33-kDa protein is essential for photooxidation of the photosynthetic metal assembly. Salt washing between pH 4.5 and 6.5 appeared to simplify the multiline signal to a 16-line pattern, suggestive of uncoupling of the manganese complex to a dinuclear complex (Section VI,B).

Flash-induced enhancements in the solvent water proton NMR relaxation rate of photosystem II particles in response to trains of one to five light flashes have been measured (281, 282). After a single flash, a strongly relaxing paramagnetic center appeared, consistent with a  $Mn(III) \rightarrow Mn(IV)$  oxidation during the advance from  $S_1$  to  $S_2$ . After a second flash, no further enhancement was found, indicating no strongly relaxing paramagnetic center was formed during the  $S_2$  to  $S_3$  transition. Indeed, no evidence for a change involving the oxidation states of the manganese could be detected for this transition. Formation of the  $S_0$  level from  $S_1$  involved the generation of a strongly relaxing paramagnetic center, as would be expected for the reduction of a trivalent manganese ion to the divalent state.

### 5. Additional Studies

Another  $S$  state, termed " $S_{-1}$ ," can be generated chemically (284). Treatment of dark-adapted spinach chloroplasts with  $H_2O_2$  followed by removal of the peroxide resulted in a two-flash delay of maximal oxygen evolution from the third flash to the fifth flash. This indicates a two-electron reduction of the  $S_1$  level occurred. As dioxygen derived from the peroxide was not detected during the first flash, the reduction must occur at the manganese center to give a complex reduced one equivalent below  $S_0$  to  $S_{-1}$ . This reduction is different from that with  $NH_2OH$  where  $N_2$  has been detected after a single flash of light (285). The formation of an  $S_{-1}$  level has also been detected in spinach PSII particles (286) and PSII complexes (287). For some species of blue-green algae, an abnormality has been noted in the pattern of oxygen

evolution during a train of flashes; this deviation from the Kok *S*-state scheme has been modeled assuming a contribution from a naturally occurring  $S_{-1}$  state (288–290). Inclusion of a state at the “ $S_{-2}$ ” level in the simulations did not improve the fit (289).

While the pattern of proton release into the lumen during a series of flashes was under debate for a considerable period of time, a consensus appears to have been reached. In 1985, Forster and Junge showed that the pattern of  $H^+$  release during the *S*-state transitions was +1, 0, +1, and +2 corresponding to the  $S_0 \rightarrow S_1$ ,  $S_1 \rightarrow S_2$ ,  $S_2 \rightarrow S_3$ , and  $S_3 \rightarrow (S_4) \rightarrow S_0$  transitions, respectively (291). This pattern was confirmed using  $NH_2OH$  treatment, which delayed the proton release pattern by two flashes (292). Two protons were released during the first flash, which may result from hydroxylamine oxidation. This first flash appeared to produce an  $S_0$  level identical to the unperturbed  $S_0$  level of the enzyme (292). Concentration dependence studies of the two-digit shift in the proton release pattern indicated that cooperative binding of three or four molecules of  $NH_2OH$  was involved (293). The measured proton release pattern may not be equal to that of the active site of the enzyme, although this is often assumed; binding to basic sites adjacent or even near the active site may occur prior to release to the lumen.

Mass spectroscopic studies of the oxidation products of chloroplasts treated with  $^{18}OH_2$  and preilluminated or illuminated with flashes of light indicated that the  $S_1$ ,  $S_2$ , and  $S_3$  levels did not contain tightly bound  $H_2O$  or bound nonexchangeable  $H_2O$  in intermediate oxidation states (294). These results suggest that  $H_2O$  oxidation occurs solely during the  $S_3 \rightarrow S_4 \rightarrow S_0$  advance; this interpretation is consistent with the difference ultraviolet absorption studies which revealed manganese oxidation during the  $S_0 \rightarrow S_1$ ,  $S_1 \rightarrow S_2$ , and  $S_2 \rightarrow S_3$  transitions (Section VI,A,2) and the appearance and disappearance of the multiline EPR signal during the  $S_1 \rightarrow S_2$  and  $S_2 \rightarrow S_3$  transitions, respectively (Section VI,A,4). If one proton is released during the  $S_0 \rightarrow S_1$  transition and water binds during the  $S_1$ -to- $S_2$  transition without being oxidized, then the proton released during the  $S_0 \rightarrow S_2$  transition cannot come directly from water and must come from an acidic site near the photosynthetic manganese assembly. The remaining protons which are released presumably would then arise from bound water. Calculations by Krishtalik (295) have shown that ionization of water molecules preceding their oxidation favors the photosynthetic reaction.

As an oxidation occurs during each of the *S*-state advances and the proton release pattern is +1, 0, +1, and +2, the  $S_2$  and  $S_3$  levels should bear a univalent positive charge compared to the  $S_0$  and  $S_1$  levels; Saygin and Witt have shown that an absorption change at 514 nm is

due to an electrochromic shift of a pigment molecule near the Mn assembly (296). This signal is maximal in the  $S_2$  and  $S_3$  levels and is believed to be indicative of a buildup of positive charge in these  $S$  states. Similar results have been obtained at other wavelengths (297). Reexamination by Dekker and van Gorkum (298) of the electrochromic shifts indicated that the charge buildup did not exactly correspond to +1; the charge distribution on the manganese complex was best represented as  $S_2 > S_3 \gg S_0 > S_1$ . These results may explain why the  $S_1$  state is so stable in the dark (298).

## B. MODEL STUDIES

The short Mn-to-ligand distance observed in EXAFS studies of the photosynthetic manganese site has been observed in manganese coordination chemistry only for complexes containing bridging oxide or hydroxide ligands. Structurally characterized Mn complexes contain a variety of types of bridging oxide and hydroxide ligation: linear  $\mu$ -oxide (173, 175, 176), bent  $\mu$ -oxide (168–170, 307), di- $\mu$ -oxide (171, 172, 174), di- $\mu$ -hydroxide (131),  $\mu_3$ -oxide (301–306, 308–310, 319–322), and  $\mu_4$ -oxide (311). Careful examination of the structural parameters of oxide- and hydroxide-bridged Mn dimers (Table IX) indicates that complexes containing a single oxide bridge, whether linear or bent, have Mn···Mn separations significantly longer than the approximately 2.7-Å distance determined in the EXAFS studies. Only di- $\mu$ -oxide (or hydroxide) bridged dimers can reproduce this short Mn···Mn distance and the Mn–O distance.

A striking similarity has been noted between the EXAFS spectrum of  $[\text{Mn}_2\text{O}_2(\text{bipy})_4]^{3+}$  and its 1,10-phenanthroline analog and the EXAFS spectrum of the photosynthetic manganese (312); the structure of this bipy complex is shown in Fig. 15 (172). Strong correspondence was found between the number, type, and distances of the first coordination sphere of the manganese from both sources. These results strongly suggest the photosynthetic metal assembly may possess a central  $\text{Mn}_2\text{O}_2$  rhomb with additional manganese at the long 3.3-Å distance from this dinuclear core or may be composed of a pair of such  $\text{Mn}_2\text{O}_2$  units with interdimer separations of  $\sim 3.3$  Å; consequently, the data seem incompatible with a highly symmetric tetranuclear structure (313). The dinuclear bipy complex has also been shown to give rise to a 16-line EPR signal, centered at approximately  $g = 2$  (314). This spectrum closely approaches the central 16 lines of the  $S_2$  multiline signal (256). The EPR signal of this complex and those of the other  $\text{Mn}_2^{\text{III,IV}}\text{O}_2$  complexes in Table IX (which also are made up of 16-line



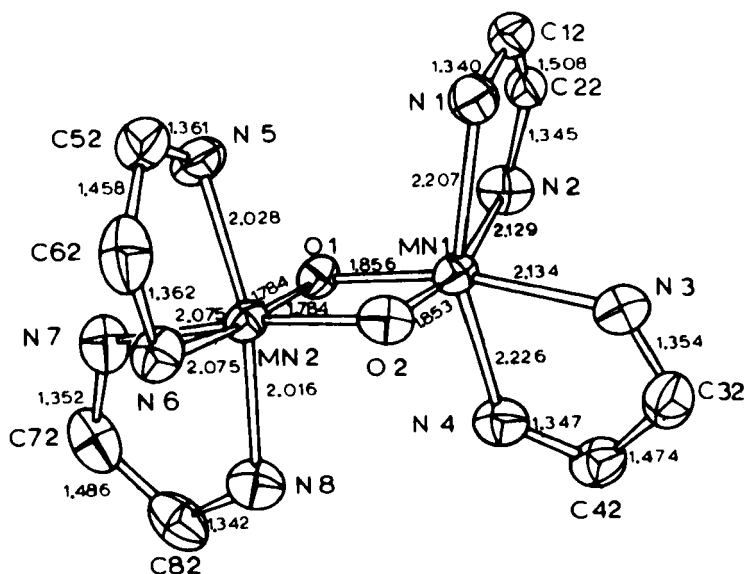


FIG. 15. The structure of  $[\text{Mn}_2\text{O}_2(\text{bipy})_4]^{3+}$ . (Reproduced with permission from Ref. 172. Copyright 1972, American Chemical Society.)

patterns) are unable to reproduce the lines in the wings of the multiline signal and have a very different temperature dependence than the PSII signal (315), possibly indicating the presence of additional manganese in the enzyme complex.

Should the WOC prove to be dinuclear (or two well-separated dinuclear units), the combined EPR and EXAFS studies suggest that the  $\text{Mn}_2\text{O}_2$ -containing complexes at the (III,IV) oxidation level would correspond to  $S_2$  and, therefore, that the (IV,IV) oxidation level would correspond to  $S_3$ . Models for the  $S_0$  and  $S_1$  states would presumably then require di- $\mu$ -oxide-bridged species at the (II,III) and (III,III) oxidation levels, respectively; no such species are currently known and must remain objectives for future work. Nevertheless, the current status of dinuclear model studies suggests that these  $\text{Mn}_2\text{O}_2$  complexes provide, at the very least, close minimal representation of the WOC, and possibly more.

The identity of the di- $\mu$ -hydroxo complex in Table IX (Fig. 16) has recently been questioned. While the original report claimed that the hydroxyl protons were located in the X-ray studies (131), an alternative structure with a  $\text{Mn(IV)}_2\text{O}_2$  core has been suggested as equally consistent with the data (316). Infrared studies favor the di- $\mu$ -hydroxide interpretation (317), however, and the true situation remains unclear.

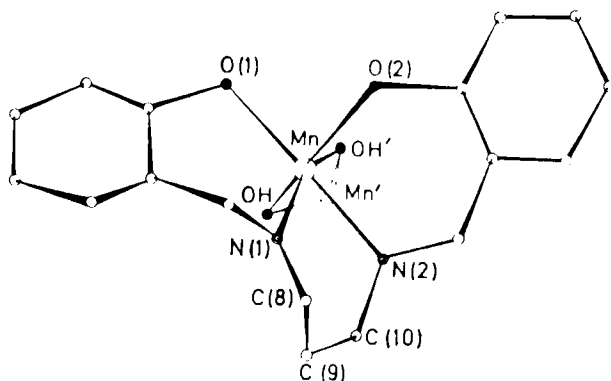


FIG. 16. The structure of  $[\text{Mn}_2(\text{OH})_2(\text{salpn})_2]$ . (Reproduced with permission from Ref. 131. Copyright 1973, Royal Society of Chemistry.)

All reported trinuclear manganese–oxide complexes possess the so-called “basic carboxylate” structure (Fig. 17) (62, 301–303). The three metals are disposed in a triangle with a central  $\mu_3$ -oxide in (or approximately in) the  $\text{Mn}_3$  plane; two carboxylates bridge each pair of Mn, while the last coordination site on each metal is filled by a terminal donor ligand such as pyridine, imidazole, or water. This arrangement

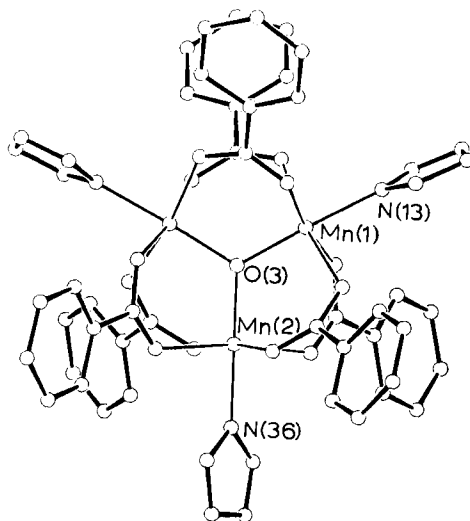


FIG. 17. The structure of  $[\text{Mn}_3\text{O}(\text{O}_2\text{CPh})_6(\text{ImH})_3]^+$ .

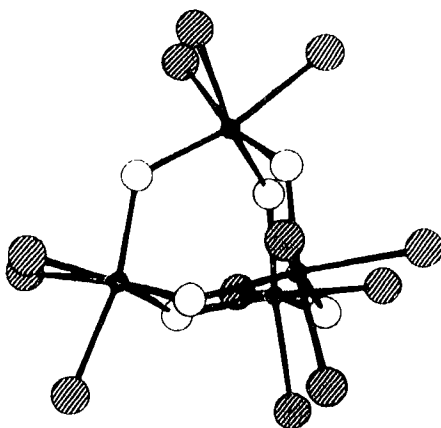


FIG. 18. The structure of  $[\text{Mn}_4\text{O}_6(\text{TACN})_4]^{4+}$ . (●) Mn, (○) O, and (⊗) N. (Reproduced with permission from Ref. 307. Copyright 1983, Verlag Chemie.)

results in all  $\text{Mn}\cdots\text{Mn}$  separations being on the order of 3.3 Å, appreciably longer than the short distance detected in the EXAFS studies. Some polymeric complexes with repeating trinuclear units similar to those described above have also been structurally characterized (305, 306).

Mn-oxide complexes composed of more than three metal centers are quite rare, only tetranuclear (307–310, 318), a single hexanuclear (311), a single nonanuclear (319, 320), and a pair of dodecanuclear (321, 322) compounds having been established to date. The first reported tetranuclear complex was  $\text{Mn}_4^{\text{IV}}\text{O}_6(\text{TACN})_4^{4+}$ , synthesized by Wieghardt and co-workers (Fig. 18) (307). The compound possesses the  $\text{Mn}_4\text{O}_6$  adamantane-type core, with all  $\text{Mn}\cdots\text{Mn}$  distances being approximately 3.21(1) Å, again too long to model the photosynthetic manganese site. The EXAFS spectrum of this complex has recently been reported (253).

In 1987, the first tetranuclear manganese-oxide complex which displayed both long and short manganese separations was reported (308, 318). Reaction of  $[\text{Mn}_3^{\text{III}}\text{O}(\text{OAc})_6(\text{py})_3]\text{ClO}_4$  with bipyridine resulted in the formation of the novel complex  $[\text{Mn}(\text{III})_4\text{O}_2(\text{OAc})_7(\text{bipy})_2]\text{ClO}_4$  (Fig. 19). The  $[\text{Mn}_4\text{O}_2]$  core of this complex has a “butterfly” arrangement of the manganese with a dihedral angle of 135.35°. The central  $\text{Mn}\cdots\text{Mn}$  distance between the hinge manganese, 2.848(5) Å, is significantly shorter than the other  $\text{Mn}\cdots\text{Mn}$  separations, 3.299(5)–3.385(5) Å. The central  $\text{MnO}_2$  rhomb is akin to that in  $[\text{Mn}_2\text{O}_2(\text{bipy})_4]^{3+}$ .

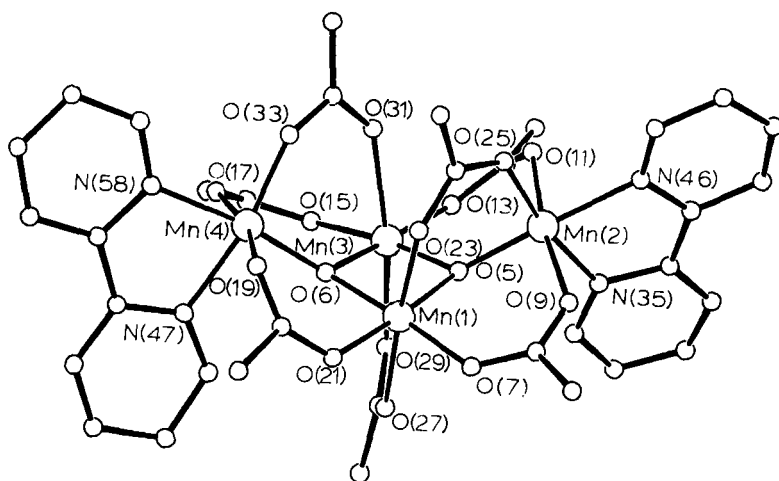


FIG. 19. The structure of  $[\text{Mn}_4\text{O}_2(\text{O}_2\text{CMe})_7(\text{bipy})_2]^+$ . (Reproduced with permission from Ref. 308. Copyright 1987, Royal Society of Chemistry.)

This complex possesses several features which are similar to those of the enzyme site and which thus make it attractive as a potential model: (1) a metal nuclearity of four; (2) oxide bridges between the metal centers and terminal O- and N-based ligation; (3) an average metal oxidation state of +3 (corresponding to that currently believed to be present in the enzyme  $S_1$  state); (4) metric parameters which are consistent with, although slightly longer than the EXAFS data on the enzyme (Table X); and (5) two pairs of inequivalent manganese. Further studies showed that analogs of the complex could be synthesized with a variety of carboxylates (318).

Extension of the bipyridine reaction to the mixed-valence triangles  $\text{Mn}_3\text{O}(\text{O}_2\text{CPh})_6(\text{py})_2(\text{H}_2\text{O})$  and  $\text{Mn}_3\text{O}(\text{OAc})_6(\text{py})_3$  resulted in the formation of the first mixed-valence tetranuclear Mn-oxide complexes,  $\text{Mn}_4\text{O}_2(\text{O}_2\text{CPh})_7(\text{bipy})_2$  (308, 318) and  $\text{Mn}_4\text{O}_2(\text{OAc})_6(\text{bipy})_2$ , containing  $\text{Mn}^{\text{II}}\text{Mn}_3^{\text{III}}$  and  $\text{Mn}_2^{\text{II}}\text{Mn}_2^{\text{III}}$ , respectively. These complexes, based on  $S_1$  containing  $\text{Mn}_4^{\text{III}}$ , would represent potential models of the  $S_0$  and  $S_{-1}$  levels of the enzyme. The acetate complex has been structurally characterized (Fig. 20 and Table X). The molecule lies on a crystallographic inversion center, resulting in an exactly planar array of four Mn atoms. The central five-coordinate Mn are the pair of trivalent ions. The distance between these manganese, 2.779(1) Å, is considerably shorter than the other Mn...Mn distances, 3.288(1) and 3.481(1) Å.

EXAFS studies (323) on the  $S_1$  model display four scattering shells, similar to the photosynthetic manganese. In an identical fashion to the

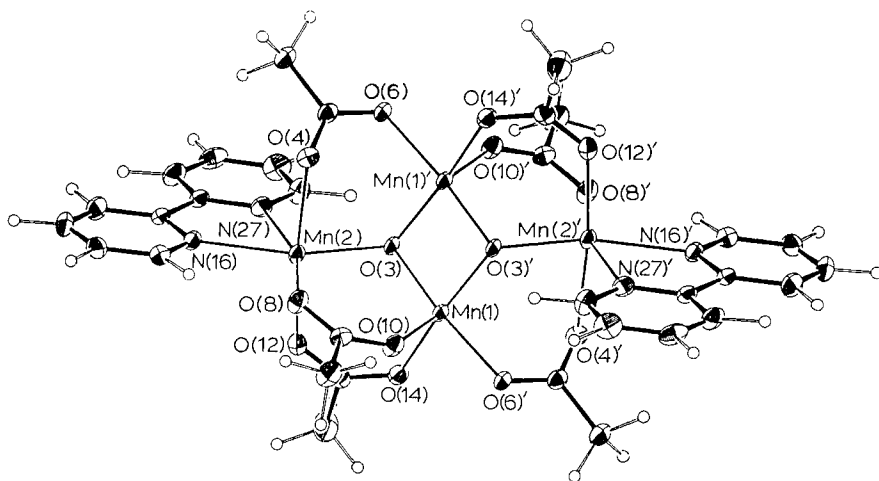
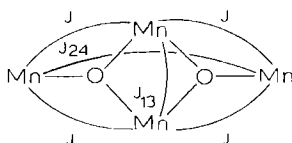


FIG. 20. The structure of  $[\text{Mn}_4\text{O}_2(\text{O}_2\text{CMe})_6(\text{bipy})_2]$ . (Reproduced with permission from Ref. 309. Copyright 1987, Royal Society of Chemistry.)

natural system,  $k$  weighting specifically labels the short and long manganese separations. Approximately 2 eV separate the edge inflection points of the  $S_0$  and  $S_1$  models, indicating that the magnitude of the  $K$ -edge shift occurring during the  $S_1$ -to- $S_2$  transition can be accounted for solely by an oxidation state change of the manganese cluster. Variable-temperature magnetic susceptibility studies on the  $\text{Mn}_4\text{O}_2$  complexes has revealed that all display weak antiferromagnetic spin exchange. Using the Hamiltonian  $H = -2J[S_3 \cdot S_4 + S_2 \cdot S_3 + S_1 \cdot S_2 + S_1 \cdot S_4] - 2J_{13}[S_3 \cdot S_1] - 2J_{24}[S_4 \cdot S_2]$  where  $J$ ,  $J_{13}$ , and  $J_{24}$  are defined as follows:



SCHEME 2.

The experimental susceptibility data can be fit to a theoretical expression involving isotropic pairwise interactions. Results are given in Table XI (318).

Cyclic voltammograms of  $[\text{Mn}_4\text{O}_2(\text{O}_2\text{CPh})_7(\text{bipy})_2]^+$  show two quasireversible processes: a reduction to  $\text{Mn}_4\text{O}_2(\text{O}_2\text{CPh})_7(\text{bipy})_2$  at  $-0.16$  V (versus ferrocene) and an oxidation to the  $\text{Mn}_4(\text{III}, \text{III}, \text{III}, \text{IV})$

TABLE XI

MAGNETIC EXCHANGE PARAMETERS ( $\text{cm}^{-1}$ ) FOR  $\text{Mn}_4\text{O}_2$  COMPLEXES

Complex	$J_{13}$	$J$	$J_{24}$	$g$
$\text{Mn(III)}_4\text{O}_2(\text{OAc})_7(\text{bipy})_2^+$	-23.5	-7.8	0	2.0
$\text{Mn}_4(3\text{III}, 2\text{II})_2(\text{O}_2\text{CPh})_7(\text{bipy})_2$	-16.6	-2.2	-0.5	1.85
$\text{Mn}_4(2\text{III}, 2\text{II})\text{O}_2(\text{OAc})_6(\text{bipy})_2$	-3.1	-2.0	0	1.67

mixed-valence complex at +0.87 V (318). Correspondingly, cyclic voltammograms of  $\text{Mn}_4\text{O}_2(\text{O}_2\text{CPh})_7(\text{bipy})_2$  showed two quasireversible waves at the same potentials. The  $S_{-1}$  model,  $\text{Mn}_4\text{O}_2(\text{OAc})_6(\text{bipy})_2$ , also exhibited quasireversible oxidation in  $\text{CH}_2\text{Cl}_2$  at -0.02 V. Thus, the tetranuclear units  $[\text{Mn}_4\text{O}_2]^{6+, 7+, 8+, 9+}$  are all interconvertible electrochemically. However, only the  $S_{-1}/S_0$  and  $S_0/S_1$  model couples had potentials within the realm of the biological system; the potential of the  $S_1/S_2$  couple was greater than that reported for the electron acceptor to the photosynthetic manganese assembly ( $\sim 1.0$  V versus NHE) (324). This indicates an additional process is necessary to reduce the potential of the  $\text{Mn}_4(\text{III}, \text{III}, \text{III}, \text{III})/(\text{III}, \text{III}, \text{III}, \text{IV})$  couple so that oxidation can occur under physiological conditions. The binding of water or ammonia during the  $S_0 \rightarrow S_1$  transition (*vide supra*) may thus facilitate the oxidation of the photosynthetic manganese center.

The difference spectrum between  $\text{Mn}_4\text{O}_2(\text{O}_2\text{CPh})_7(\text{bipy})_2^+$  and  $\text{Mn}_4\text{O}_2(\text{O}_2\text{CPh})_7(\text{bipy})_2$  has also been reported. The spectrum is strikingly similar in shape to the spectrum determined recently for the  $S_0 \rightarrow S_1$  transition (Fig. 21) (318).

A unique tetranuclear manganese complex with a cubane-type core has recently been synthesized and characterized (310). The anion  $[\text{Mn}_4\text{O}_3\text{Cl}_6(\text{HIm})(\text{OAc})_3]^{2-}$  represents the first structurally characterized manganese species with an average oxidation level corresponding to that thought present at the  $S_2$  state of the water oxidation center (Fig. 22 and Table X). This compound also possesses two distinct  $\text{Mn} \cdots \text{Mn}$  separations: a short distance averaging  $\sim 2.8$  Å and a long distance averaging  $\sim 3.3$  Å.

The most beneficial aspect of the complex is that it allows for the first time the observation of an EPR signal for a tetranuclear manganese complex at the oxidation level believed to correspond to that which gives rise to the multiline EPR signal. X-Band spectra of the complex as a DMF/toluene glass displayed signals at  $g \approx 9$ ,  $\sim 6$ , and  $\sim 4$ , as well as a  $g \approx 2$  signal. The latter contains at least 16 well-defined hyperfine lines. Magnetic susceptibility data revealed that on cooling

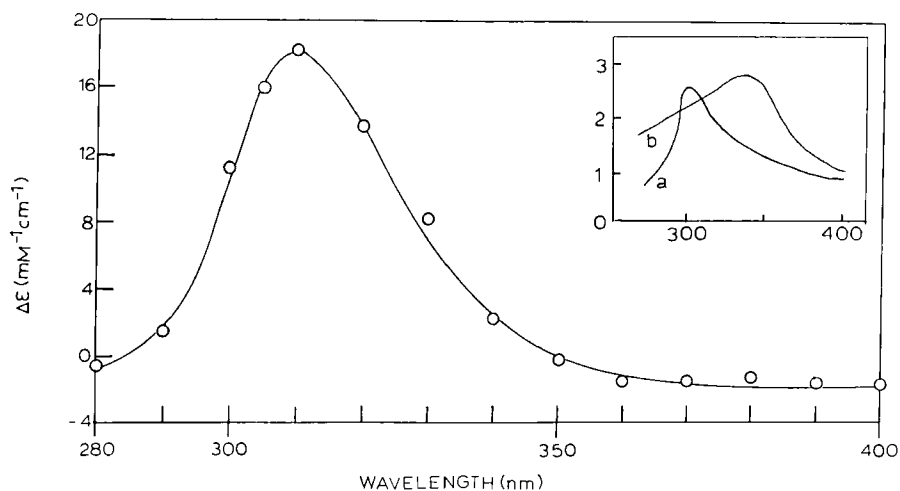


FIG. 21. Difference absorbance spectra for  $[\text{Mn}_4\text{O}_2(\text{O}_2\text{CPh})_7(\text{bipy})_2]^{0,+}$ . The inset is Fig. 13, for comparison.

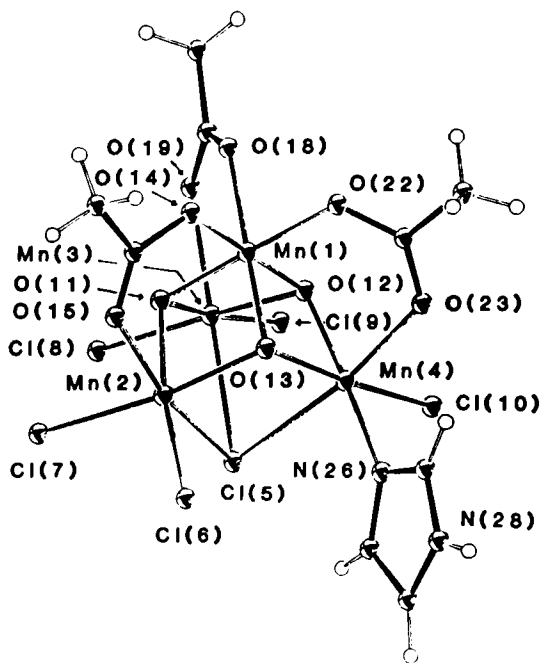


FIG. 22. The structure of  $[\text{Mn}_4\text{O}_3\text{Cl}_6(\text{O}_2\text{CMe})_3(\text{ImH})]^{2-}$ . (Reproduced with permission from Ref. 310. Copyright 1987, American Chemical Society.)

from 300 to 60 K, the magnetic moment per molecule increased from 8.82 to 9.54  $\mu_B$ . Below these temperatures,  $\mu_{\text{eff}}$  dropped until, at 5 K, the magnetic moment was 7.16  $\mu_B$ . In addition to this complex, a pyridine analog has recently been characterized by X-ray techniques, and its magnetic and spectral properties are under investigation (325).

### C. PROPOSED MECHANISMS FOR WATER OXIDATION

Two mechanisms for photosynthetic water oxidation invoking structurally characterized tetranuclear manganese units have been put forward recently. The first, proposed by Brudvig and Crabtree (326)

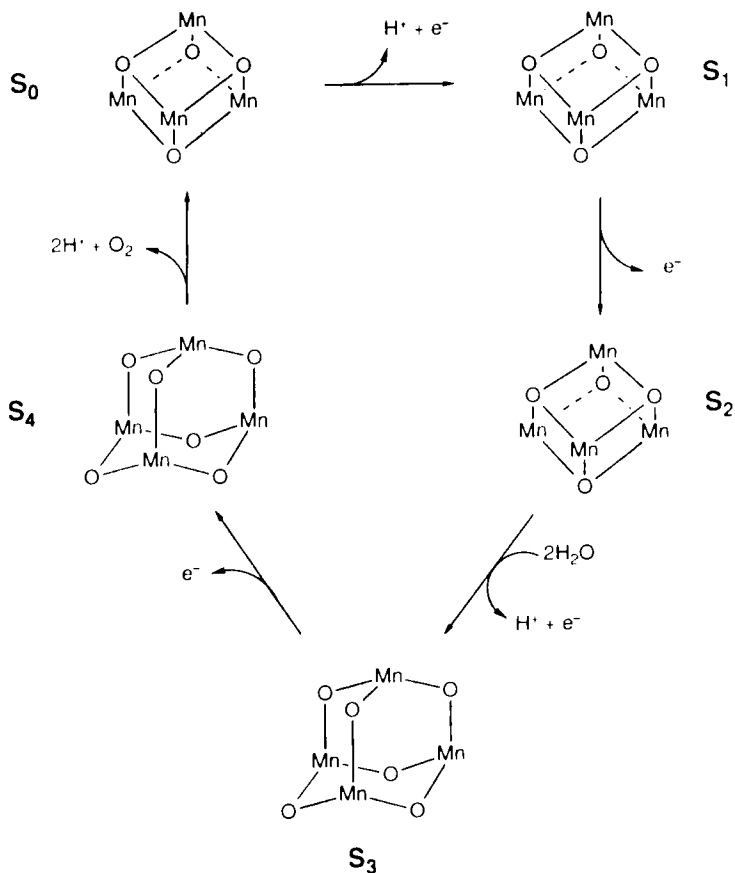


FIG. 23. Schematic representation of cubane/adamantane mechanism of water oxidation. (Reproduced with authors' permission from Ref. 326.)



in 1986, utilizes a “ $\text{Mn}_4\text{O}_6$  adamantane”-like complex and a “ $\text{Mn}_4\text{O}_4$  cubane”-like assembly (Fig. 23). In this scheme, a Jahn–Teller distorted cubane is oxidized during the  $S_0 \rightarrow S_1$  and  $S_1 \rightarrow S_2$  transitions. However, during the  $S_2 \rightarrow S_3$  advance, two molecules of water are incorporated into the cubane-like structure which rearranges to give an  $\text{Mn}_4\text{O}_6$  adamantane complex. On further oxidation, an O–O bond forms from two of the bridging oxides, and the  $\text{O}_2$  is subsequently released. Three possible schemes for the manganese oxidation states at each  $S$  level were presented. The one considered most likely was  $S_0$ , 3Mn(III), Mn(IV);  $S_1$ , 2Mn(III), 2Mn(IV);  $S_2$ , 3Mn(IV), Mn(III);  $S_3$ , 4Mn(IV); and  $S_4$ , 3Mn(IV), Mn(V).

The second scheme, the “double-pivot” mechanism proposed by Vincent and Christou (304), was reported in 1987. This mechanism for the water oxidation cycle is shown in Fig. 24. During the  $S_0 \rightarrow S_1$  and  $S_1 \rightarrow S_2$  transitions, an  $\text{Mn}_4\text{O}_2$  butterfly is oxidized without any structural rearrangement. Concurrent with the  $S_1 \rightarrow S_2$  advance, two

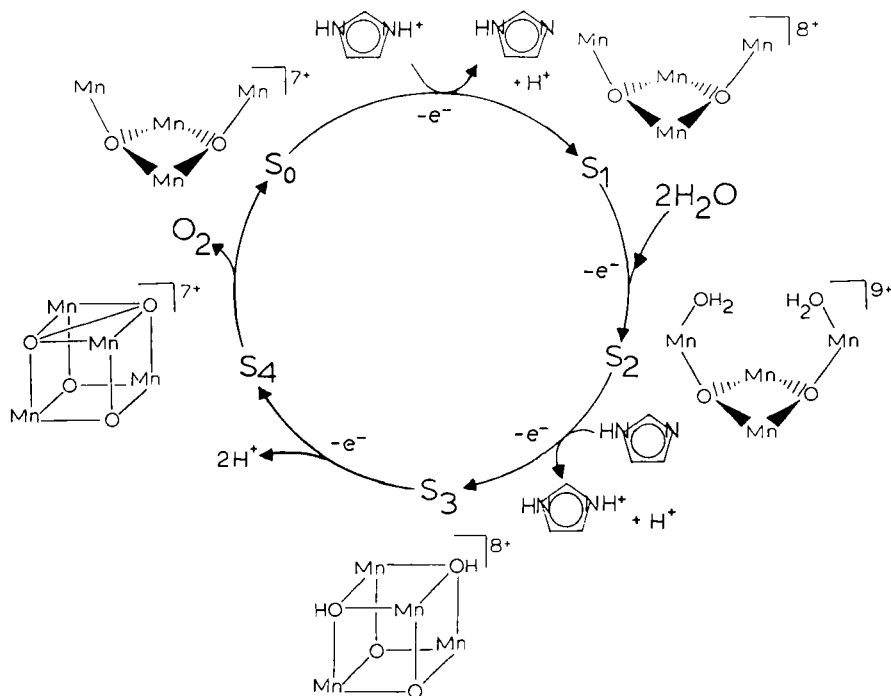


FIG. 24. Schematic representation of the “double-pivot” mechanism of water oxidation. (Reproduced with permission from Ref. 304. Copyright 1987, Elsevier Sequoia.)

molecules of water are bound to the "wingtip" manganese sites. Further oxidation from  $S_2 \rightarrow S_3$  then results in the structural rearrangement tentatively suggested by EXAFS studies (254). Movement of the two "wingtip" manganese toward each other occurs by pivoting of the Mn–O vectors about the  $\mu_3$ -O atoms; this "double-pivot" maneuver requires no movement in the  $Mn_2O_2$  base, but merely an increase in the "pyramidity" of the  $\mu_3$ -O atoms. Concomitant deprotonation of the water to  $OH^-$  allows the unit to convert to a more compact structure. Formation of  $\mu_3$ -OH $^-$  bridges produces a cubane-like structure. Oxidation of  $S_3 \rightarrow S_4$  now triggers the substrate oxidation process. The oxygen atoms derived from water move toward each other, initiating bond formation, and there is concomitant movement apart of the two manganese atoms and transfer of electrons to Mn. An intermediate in this concerted reaction might be a peroxide-bound form as shown. The following oxidation states at each  $S_n$  level were favored by the authors:  $S_0$ , Mn(II), 3Mn(III);  $S_1$ , 4Mn(III);  $S_2$ , 3Mn(III), Mn(IV); and  $S_3$ , 2Mn(III), 2Mn(IV). The  $H^+$  release pattern is also addressed in this scheme, which involves an imidazole moiety of a histidine residue to keep charge balance.

Since the latter proposal was published, the synthesis of the  $Mn_4O_3$ -containing complex (Fig. 22) has suggested a possible modification. It is interesting that the  $Mn_4O_3$  core is merely the  $Mn_4O_2$  "butterfly" unit with an additional  $\mu_3$ -O $^{2-}$  bridging the two "wingtip" and one of the "hinge" Mn atoms. This suggests that an  $Mn_4O_3$  core could replace the proposed structure at  $S_2$ , the third O $^{2-}$  derived from a  $H_2O$  molecule. This possibly requires that  $H_2O$  binding to the photosynthetic manganese site occurs sequentially, with the first molecule of water being attached during the oxidation of  $S_1 \rightarrow S_2$  and the second being bound during the following transition. Velthuys, in his studies of ammonia binding, has discussed the possibility of sequential substrate binding (274). Additionally (as mentioned previously), dimers containing the  $Mn(III)_2O(OAc)_2^{2+}$  core readily hydrolyze in aerobic aqueous solution to new dimeric compounds with oxidized cores,  $Mn_2(III, IV)O_2(OAc)_2^{2+}$ . However, the charge on the core units remains constant. This suggests that the mechanism which reduces the potential of the photosynthetic manganese assembly toward oxidation may involve such a carboxylate replacement by oxide (or hydroxide). This type of exchange would be perfectly in line with the possibility of stepwise binding of  $H_2O$  and the folding up of the manganese assembly on oxidation in the proposed "double-pivot" mechanism and its described modification. Bridging carboxylate by bridging hydroxide exchange has been observed in cobalt-oxide complexes of the "basic carboxylate"-type structure (299). Saygin *et al.* (300) have shown that incubation of PSII particles

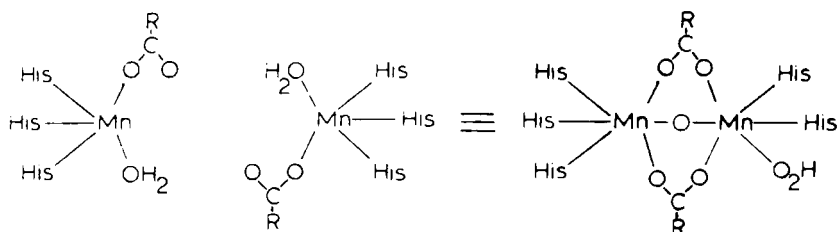
with acetate reversibly deactivates the oxygen-evolving system. It may be that excess acetate thus inhibits the oxide-for-carboxylate exchange required for conversion of  $\text{Mn}_4\text{O}_2$  units to  $\text{Mn}_4\text{O}_3$  and  $\text{Mn}_4\text{O}_4$  at the higher  $S_n$  states.

## VII. Concluding Remarks

We have attempted to survey both the current status of studies attempting to elucidate the nature of higher oxidation Mn biomolecules, and the efforts directed toward the synthesis of satisfactory inorganic models. As we noted in Section I, this is consequently by no means an exhaustive account of all the work reported, and references to more detailed reviews of specific systems have been cited in the text. Nor have all Mn-containing or Mn-dependent biological systems been included; again, more detailed and exhaustive reviews are available elsewhere (327).

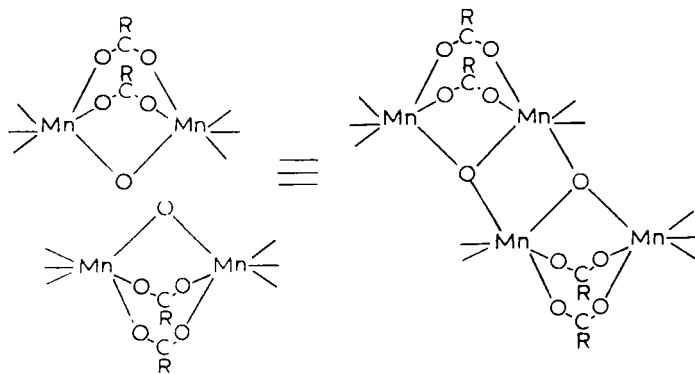
It is interesting that, with the exception of acid phosphatase and transferrin, all the biological systems discussed are involved in the same basic function, viz. interconversion of oxygen among its various oxidation states. Thus, these Mn enzymes are involved in superoxide dismutation to  $\text{O}_2$  and  $\text{O}_2^{2-}$  (a one-electron process), peroxide disproportionation to  $\text{O}_2$  and  $\text{H}_2\text{O}$  (a two-electron process), and water oxidation to  $\text{O}_2$  (a four-electron process). It is perhaps coincidental, but also perhaps of evolutionary significance, that these systems employ mononuclear, dinuclear, and (probably) tetranuclear sites, respectively. Given that nature is often found to be quite conservative, maximizing the utility of a given prosthetic group such as the ubiquitous Fe protoporphyrin IX unit, one wonders whether the Mn SOD, catalase, and the WOC have a common ancestor which has diverged to provide greater specificity and catalytic efficiency in the various "oxygen-transformation" reactions described. With this in mind, we detail to the reader the following structural interrelationship between the SOD and proposed catalase Mn sites, and the catalase and proposed WOC Mn sites.

The hemerythrin-like  $\text{Mn}_2\text{O}(\text{O}_2\text{CR})_2$  site bears striking resemblance to the result of fusing two mononuclear SOD Mn sites, as depicted in Scheme 3. Could the need for a system readily capable of sustaining two-electron processes have resulted in the evolutionary merging of two one-electron systems? A similar argument can be made for the mononuclear site of Fe SOD (isostructural to Mn SOD) (27) and hemerythrin. Similarly, the  $\text{Mn}_4\text{O}_2$  units proposed as models for the active site of the photosynthetic WOC can result from fusion of two



SCHEME 3.

$\text{Mn}_2\text{O}(\text{O}_2\text{CR})_2$  units as shown in Scheme 4. Again, could the requirement for a system capable of four-electron processes have led to the evolutionary merging of two two-electron systems? If so, again it may be more than coincidence that the WOC is capable of functioning as a catalase when  $\text{O}_2$  evolution is blocked (287) but merely a reflection of the intrinsic properties of the dinuclear catalase-like unit which forms its substructure and represents its evolutionary ancestor.



SCHEME 4.

## REFERENCES

1. Keele, B. B., Jr., McCord, J. M., and Fridovich, I., *J. Biol. Chem.* **245**, 6176 (1970).
2. Ose, D. E., and Fridovich, I., *J. Biol. Chem.* **251**, 1217 (1976).
3. Dingle, R., *Acta Chem. Scand.* **20**, 30 (1966).
4. Fee, J. A., Shapiro, E. R., and Moss, T. H., *J. Biol. Chem.* **251**, 6157 (1976).
5. Fernandez, V. M., Sevilla, F., Lopez-Gorge, J., and del Rio, L. A., *J. Inorg. Biochem.* **16**, 79 (1982).
6. Reinards, R., Altdorf, R., and Ohlenbusch, H.-D., *Hoppe-Seyler's Z. Physiol. Chem.* **365**, 577 (1984).

7. Sato, S., and Harris, J. I., *Eur. J. Biochem.* **73**, 373 (1977).
8. Sato, S., and Nakazawa, K., *J. Biochem. (Tokyo)* **83**, 1165 (1978).
9. Lumsden, J., Cammack, R., and Hall, D. O., *Biochim. Biophys. Acta* **438**, 380 (1976).
10. Lavelle, F., Durosay, P., and Michelson, A. M., *Biochimie* **56**, 451 (1974).
11. Ravindranath, S. D., and Fridovich, I., *J. Biol. Chem.* **250**, 6107 (1975).
12. Vance, P. G., Keele, B. B., Jr., and Rajagopalan, K. V., *J. Biol. Chem.* **247**, 4782 (1972).
13. Harris, J. T., in "Superoxide and Superoxide Dismutases" (J. M. Michelson, J. M. McCord, and I. Fridovich, eds.), p. 151. Academic Press, New York, 1977.
14. Weisinger, R. A., and Fridovich, I., *J. Biol. Chem.* **248**, 3582 (1973).
15. Salin, M. L., Day, E. D., and Crapo, J. D., *Arch. Biochem. Biophys.* **187**, 223 (1978).
16. Abe, Y., and Okazaki, T., *Arch. Biochem. Biophys.* **253**, 241 (1987).
17. McCord, J. M., Boyle, J. A., Day, E. D., Jr., Rizzolo, L. J., and Salin, M. L., in "Superoxide and Superoxide Dismutases" (A. M. Michelson, J. M. McCord, and I. Fridovich, eds.), p. 129. Academic Press, New York, 1977.
18. Ravindranath, S. D., and Fridovich, I., *J. Biol. Chem.* **250**, 6107 (1975).
19. Meier, B., Barra, D., Bossa, F., Calabrese, L., and Rotilo, G., *J. Biol. Chem.* **257**, 13977 (1982).
20. Ichihara, K., Kusunose, E., Kusunose, M., and Mori, T., *J. Biochem. (Tokyo)* **81**, 1427 (1977).
21. Misra, H. P., and Fridovich, I., *J. Biol. Chem.* **252**, 6421 (1977).
22. Brock, C. J., Harris, J. I., and Sato, S., *J. Mol. Biol.* **107**, 175 (1976).
23. Brock, C. J., and Harris, J. I., *Biochem. Soc. Trans.* **5**, 1537 (1977).
24. Kusunose, M., Noda, Y., Ichihara, K., and Kusunose, E., *Arch. Microbiol.* **108**, 65 (1976).
25. Terech, A., and Vignais, P. M., *Biochim. Biophys. Acta* **657**, 411 (1981).
26. Sevilla, F., Lopez-Gorge, J., and del Rio, L. A., *Planta* **150**, 153 (1980).
27. Stallings, W. C., Pattridge, K. A., Strong, R. K., and Ludwig, M. L., *J. Biol. Chem.* **259**, 10695 (1984).
28. Beem, K. M., Richardson, J. S., and Richardson, D. C., *J. Mol. Biol.* **105**, 327 (1976).
29. Bridgen, J., Harris, J. I., and Kolb, E., *J. Mol. Biol.* **105**, 333 (1976).
30. Marklund, A., *Int. J. Biochem.* **9**, 299 (1978).
31. Lavelle, F., and Michelson, A. M., *Biochimie* **57**, 375 (1975).
32. Beaman, B. L., Scates, S. M., Moring, S. E., Deem, R., and Misra, H. P., *J. Biol. Chem.* **258**, 91 (1983).
33. Stallings, W. C., Powers, T. B., Pattridge, K. A., Fee, J. A., and Ludwig, M. L., *Proc. Natl. Acad. Sci. U.S.A.* **80**, 3884 (1983).
34. Steinman, H. M., and Hill, R. L., *Proc. Natl. Acad. Sci. U.S.A.* **70**, 3725 (1973).
35. Barra, D., Schinina, M. E., Bossa, F., and Bannister, J. V., *FEBS Lett.* **179**, 329 (1985).
36. Moody, C. S., and Hassen, H. M., *J. Biol. Chem.* **259**, 12821 (1984).
37. Martin, M. E., Byers, B. R., Olson, M. O. J., Salin, M. L., Arceneaux, J. E. L., and Tolbert, C., *J. Biol. Chem.* **261**, 9361 (1986).
38. Bannister, J. V., and Rotilio, G., in "The Biology and Chemistry of Active Oxygen" (J. V. Bannister and W. H. Bannister, eds.), p. 146. Am. Elsevier, New York, 1984.
39. Parker, M. W., Schinina, M. E., Bossa, F., and Bannister, J. V., *Inorg. Chim. Acta* **91**, 307 (1984).
40. Stallings, W. C., Pattridge, K. A., Strong, R. K., and Ludwig, M. L., *J. Biol. Chem.* **260**, 16424 (1985).
41. Villafranca, J. J., Yost, F. J., Jr., and Fridovich, I., *J. Biol. Chem.* **249**, 3532 (1974).
42. Boucher, L. J., and Day, V. W., *Inorg. Chem.* **16**, 1360 (1977).
43. Bernal, J., Elliot, N., and Lalancetto, R., *J. Chem. Soc., Chem. Commun.* 803 (1971).
44. Sato, S., Nakada, Y., and Nakazawa-Tomizawa, K., *Biochim. Biophys. Acta* **912**, 178 (1987).

45. Ditlow, C., Johansen, J. T., Martin, B. M., and Ivendsen, I. B., *Carlsberg Res. Commun.* **47**, 81 (1982).
46. Steinman, H. M., *J. Biol. Chem.* **253**, 8708 (1978).
47. Barra, D., Schinina, M. E., Simmaco, M., Bannister, J. V., Bannister, W. H., Rotilio, G., and Bossa, F., *J. Biol. Chem.* **259**, 12595 (1984).
48. Brock, C. J., and Walker, J. E., *Biochemistry* **19**, 2873 (1980).
49. Takeda, Y., and Avila, H., *Nucleic Acids Res* **14**, 4577 (1986).
50. Bannister, J. V., Desideri, A., and Rotilio, G., *FEBS Lett.* **188**, 91 (1985).
51. Weisiger, R. A., and Fridovich, I., *J. Biol. Chem.* **248**, 4793 (1973).
52. Hayakawa, T., Kanematsu, S., and Asada, K., *Planta* **166**, 111 (1985).
53. Bridgen, J., Harris, J. I., and Northrop, F., *FEBS Lett.* **49**, 392 (1975).
54. Fridovich, I., *Life Sci.* **14**, 819 (1974).
55. Forman, H. J., and Fridovich, I., *Arch. Biochem. Biophys.* **158**, 396 (1973).
56. Fridovich, I., *Science* **201**, 875 (1978).
57. Pick, M., Rabani, J., Yost, F., and Fridovich, I., *J. Am. Chem. Soc.* **96**, 7329 (1974).
58. McAdam, M. E., Fox, P. A., Lavelle, F., and Fielden, E. M., *Biochem. J.* **165**, 71 (1977).
59. Hallewell, R. A., Mullenbach, G. T., Stempien, M. M., and Bell, G. I., *Nucleic Acids Res.* **14**, 9539 (1986).
60. Van Atta, R. B., Strouse, C. E., Hanson, L. K., and Valentine, J. S., *J. Am. Chem. Soc.* **109**, 1425 (1987).
61. Landrum, J. T., Hatano, K., Scheidt, W. R., and Reed, C. A., *J. Am. Chem. Soc.* **102**, 6729 (1980).
62. Christmas, C., Vincent, J. B., Huffman, J. C., and Christou, G., unpublished results.
63. Phillips, F. L., Shreeve, F. M., and Skapski, A. C., *Acta Crystallogr. Sect. B* **B32**, 687 (1976).
64. Koppenol, W. H., Levine, F., Hatmaker, T. L., Epp, J., and Rush, J. D., *Arch. Biochem. Biophys.* **251**, 594 (1986).
65. Yamaguchi, K. S., Spencer, L., and Sawyer, D. T., *FEBS Lett.* **197**, 249 (1986).
66. Archibald, F. S., and Fridovich, I., *Arch. Biochem. Biophys.* **214**, 452 (1982).
67. Uehara, K., Fujimoto, S., and Taniguchi, T., *J. Biochem. (Tokyo)* **70**, 183 (1971).
68. Uehara, K., Fujimoto, S., and Taniguchi, T., *J. Biochem. (Tokyo)* **75**, 627 (1974).
69. Uehara, K., Fujimoto, S., Taniguchi, T., and Nakai, K., *J. Biochem. (Tokyo)* **75**, 639 (1974).
70. Fujimoto, S., O'Hara, A., and Uehara, K., *Agric. Biol. Chem.* **44**, 1659 (1980).
71. Fujimoto, S., Nakagawa, T., Ishimitsu, S., and Ohara, A., *Chem. Pharm. Bull.* **25**, 1459 (1977).
72. Igaue, I., Watabe, H., Takahashi, K., Takekoshi, M., and Morota, A., *Agric. Biol. Chem.* **40**, 823 (1976).
73. Fujimoto, S., Nakagawa, T., and Ohara, A., *Agric. Biol. Chem.* **41**, 599 (1977).
74. Fujimoto, S., Nakagawa, T., and Ohara, A., *Chem. Pharm. Bull.* **25**, 3283 (1977).
75. Fujimoto, S., Nakagawa, T., and Ohara, A., *Chem. Pharm. Bull.* **27**, 545 (1979).
76. Sugiura, Y., Kawabe, H., and Tanaka, H., *J. Am. Chem. Soc.* **102**, 6581 (1980).
77. Sugiura, Y., Kawabe, H., Tanaka, H., Fujimoto, S., and Ohara, A., *J. Am. Chem. Soc.* **103**, 963 (1981).
78. Sugiura, Y., Kawabe, H., Tanaka, H., Fujimoto, S., and Ohara, A., *J. Biol. Chem.* **256**, 10664 (1981).
79. Kawabe, H., Sugiura, Y., and Tanaka, H., *Biochem. Biophys. Res. Commun.* **103**, 327 (1981).
80. Kawabe, H., Sugiura, Y., Terauchi, M., and Tanaka, H., *Biochim. Biophys. Acta* **784**, 81 (1984).
81. Fujimoto, S., Murakawi, K., and Ohara, A., *J. Biochem. (Tokyo)* **97**, 1777 (1985).

82. Davis, J. C., Lin, S. S., and Averill, B. A., *Biochemistry* **20**, 4062 (1981).
83. Beck, J. L., McConachie, L. A., Summors, A. C., Arnold, W. N., DeJersey, J., and Zerner, B., *Biochim. Biophys. Acta* **869**, 61 (1986).
84. Hefler, S. K., and Averill, B. A., *Biochem. Biophys. Res. Commun.* **146**, 1173 (1987).
85. Stults, B. R., Day, R. O., Marianelli, R. S., and Day, V. W., *Inorg. Chem.* **18**, 1847 (1979).
86. Henkel, G., Greiwe, K., and Krebs, B., *Angew. Chem., Int. Ed. Engl.* **24**, 117 (1985).
87. Butcher, R. J., and Sinn, E., *J. Chem. Soc., Dalton Trans.* 2517 (1975); *J. Am. Chem. Soc.* **98**, 5159 (1976).
88. Elliot, R. L., West, B. O., Snow, M. R., and Tiekin, E. R. T., *Acta Crystallogr., Sect. C* **C42**, 763 (1986).
89. Healy, P. C., and White, A. H., *J. Chem. Soc., Dalton Trans.* 1883 (1972).
90. Brown, K. L., Golding, R. M., Healy, P. C., Jessop, K. J., and Tennant, W. C., *Aust. J. Chem.* **27**, 2075 (1974).
91. Christou, G., and Huffman, J. C., *J. Chem. Soc., Chem. Commun.* 558 (1983).
92. Costa, T., Dorfman, J. R., Hagen, K. S., and Holm, R. H., *Inorg. Chem.* **22**, 4091 (1983).
93. Seela, J. L., Huffman, J. C., and Christou, G., *J. Chem. Soc., Chem. Commun.* 58 (1985).
94. Seela, J. L., Huffman, J. C., Christou, G., Chang, H.-R., and Hendrickson, D. N., unpublished.
95. Seela, J. L., Folting, K., Wang, R.-J., Huffman, J. C., Christou, G., Chang, H.-R., and Hendrickson, D. N., *Inorg. Chem.* **24**, 4454 (1985).
96. Bashkino, J. S., Huffman, J. C., and Christou, G., *J. Am. Chem. Soc.* **108**, 5038 (1986).
97. Tatsuno, Y., Saeki, Y., Iwaki, M., Yagi, T., Nozaki, M., Kitagawa, T., and Otsuka, S., *J. Am. Chem. Soc.* **100**, 4614 (1978).
98. Gaber, B. P., Sheridan, J. P., Bazer, F. W., and Roberts, R. M., *J. Biol. Chem.* **254**, 8340 (1979).
99. Holm, R. H., and Ibers, J. A., in "Iron-Sulfur Proteins" (W. Lovenberg, ed.), p. 205. Academic Press, New York, 1977.
100. Fikar, R., Koch, S. A., and Miller, M. M., *Inorg. Chem.* **24**, 3311 (1985).
101. Mukherjee, R. N., Rao, C. P., and Holm, R. H., *Inorg. Chem.* **25**, 2979 (1986).
102. Strothkamp, K. G., and Lippard, S. J., *Acc. Chem. Res.* **15**, 318 (1982), and references therein.
103. Seela, J. L., and Christou, G., unpublished results.
104. Tomimatsu, Y., Kind, S., and Scherer, J. R., *Biochemistry* **15**, 4918 (1976).
105. Mn(III)-biphenoxide complexes do however contain infrared bands in this region. Schake, A., Vincent, J. B., and Christou, G., unpublished results.
106. Fujimoto, S., Yamada, K., Kuroda, T., Tanaka, T., and Ohara, A., *Nippon Nogei Kagaku Kaishi* **60**, 605 (1986).
107. Feeney, R. E., and Komatsu, S. K., *Struct. Bonding (Berlin)* **1**, 149 (1966).
108. Aisen, P., and Listowsky, I., *Annu. Rev. Biochem.* **49**, 357 (1980).
109. Aisen, P., and Brown, E. B., *Prog. Hematol.* **9**, 25 (1975).
110. Brock, J. H., *Top. Mol. Struct. Biol.* **7**, 183 (1985).
111. Anderson, B. F., Baker, H. M., Dodson, E. J., Norris, G. E., Rumball, S. V., Waters, J. M., and Baker, E. N., *Proc. Natl. Acad. Sci. U.S.A.* **84**, 1769 (1987).
112. Zweier, J. L., and Aisen, P., *J. Biol. Chem.* **252**, 6090 (1977).
113. Teuwissen, B., Masson, P. L., Osinski, P., and Heremans, J. F., *Eur. J. Biochem.* **31**, 239 (1972).
114. Rogers, T. B., Gold, R. A., and Feeney, R. E., *Biochemistry* **16**, 2299 (1977).
115. Garrett, R. C., Evans, R. W., Hasnain, S. S., and Lindley, P. F., *Biochem. J.* **233**, 479 (1986).
116. Gaber, B. P., Schillinger, W. E., Koenig, S. H., and Aisen, P., *J. Biol. Chem.* **245**, 4251 (1970).

117. Najarian, R. C., Harris, D. C., and Aisen, P., *J. Biol. Chem.* **253**, 38 (1978).
118. Inman, J. K., Ph.D. Dissertation in Biochemistry, Division of Medical Sciences, Harvard University, Cambridge, Massachusetts, 1956.
119. Ulmer, D. D., and Vallee, B. L., *Biochemistry* **2**, 1335 (1963).
120. Aisen, P., Aasa, R., and Redfield, A. G., *J. Biol. Chem.* **244**, 4628 (1969).
121. Ainscough, E. W., Brodie, A. M., and Plowman, J. E., *Inorg. Chim. Acta* **33**, 149 (1979).
122. Ainscough, E. W., Brodie, A. M., Plowman, J. E., Bloor, S. J., Loehr, J. S., and Loehr, T. M., *Biochemistry* **19**, 4072 (1980).
123. O'Hara, P., Yeh, S. M., Meares, C. F., and Bersohn, R., *Biochemistry* **20**, 4704 (1981).
124. Keefer, R. C., Barak, A. J., and Boycott, J. D., *Biochim. Biophys. Acta* **221**, 390 (1970).
125. Hancock, R. G. V., Evans, D. J. R., and Fritze, K., *Biochim. Biophys. Acta* **320**, 486 (1973).
126. Gibbons, R. A., Dixon, S. N., Hallis, K. Russell, A. M., Sansom, B. F., and Symonds, R. W., *Biochim. Biophys. Acta* **444**, 1 (1976).
127. Scheuhammer, A. M., and Cherian, M. G., *Biochim. Biophys. Acta* **840**, 163 (1985).
128. Davies, J. E., Gatehouse, B. M., and Murray, K. S., *J. Chem. Soc., Dalton Trans.* 2523 (1973).
129. Kessissoglou, D. P., Butler, W. M., and Pecoraro, V. L., *J. Chem. Soc., Chem. Commun.* 1253 (1986).
130. Mangia, A., Nardello, M., Pelizzi, C., and Pelizzi, G., *J. Chem. Soc., Dalton Trans.* 1141 (1973).
131. Maslen, H. S., and Water, T. N., *J. Chem. Soc., Chem. Commun.* 760 (1973).
132. Mikuriya, M., Torihara, N., Okawa, H., and Kida, S., *Bull. Chem. Soc. Jpn.* **54**, 1063 (1981).
133. Raston, C. L., White, A. H., and Willis, A. C., *J. Chem. Soc., Dalton Trans.* 1793 (1974).
134. Tamura, Q., Ogawa, K., Sakurai, T., and Nakahara, A., *Acta Chim. Acta* **92**, 107 (1984).
135. Akhtar, F., and Drew, M. G. B., *Acta Crystallogr., Sect. B* **B38**, 612 (1982).
136. Chin, D.-H., Sawyer, D. T., Schaefer, W. P., and Simmons, C. J., *Inorg. Chem.* **22**, 752 (1983).
137. Hartman, J. R., Foxman, B. M., and Cooper, S. R., *Inorg. Chem.* **23**, 1381 (1984).
138. Larsen, S. K., Pierpoint, C. G., DeMunno, G., and Dolcetti, G., *Inorg. Chem.* **25**, 4828 (1986).
139. Lynch, M. W., Hendrickson, D. N., Fitzgerald, B. J., and Cortland, G., *J. Am. Chem. Soc.* **106**, 2041 (1984).
140. Vincent, J. B., Folting, K., Huffman, J. C., and Christou, G., *Inorg. Chem.* **24**, 996 (1986).
141. Pavacik, P. S., Huffman, J. C., and Christou, G., *J. Chem. Soc., Chem. Commun.* 43 (1986).
142. Nicholson, J. R., Vincent, J. B., Huffman, J. C., and Christou, G., unpublished results.
143. Schake, A., Vincent, J. B., Huffman, J. C., and Christou, G., in preparation.
144. Horvath, B., Moseler, R., and Horvath, E. G., *Z. Anorg. Allg. Chem.* **41**, 449 (1979).
145. Arndt, D., "Manganese Compounds as Oxidizing Agents in Organic Chemistry" and references therein. Open Court Publishing Co., LaSalle, Illinois, 1981.
146. Glenn, J. K., and Gold, M. H., *Arch. Biochem. Biophys.* **242**, 329 (1985).
147. Glenn, J. K., Akileswaran, L., and Gold, M. H., *Arch. Biochem. Biophys.* **251**, 688 (1986).
148. Paszczynski, A., Huynh, V.-B., and Crawford, R., *Arch. Biochem. Biophys.* **244**, 750 (1986).
149. Leisola, M. S. A., Kozulic, B., Meussdoerffer, F., and Fiechter, A., *J. Biol. Chem.* **262**, 419 (1987).



150. Archibald, F. S., and Fridovich, I., *J. Bacteriol.* **145**, 442 (1981).
151. Archibald, F. S., and Fridovich, I., *J. Bacteriol.* **146**, 928 (1981).
152. Archibald, F. S., and Fridovich, I., *Arch. Biochem. Biophys.* **215**, 589 (1982).
153. Archibald, F. S., and Fridovich, I., *Arch. Biochem. Biophys.* **214**, 452 (1982).
154. Delwiche, E. A., *J. Bacteriol.* **81**, 416 (1961).
155. Johnston, M. A., and Delwiche, E. A., *J. Bacteriol.* **83**, 936 (1962).
156. Jones, D., Deibel, D. H., and Niven, C. F., Jr., *J. Bacteriol.* **88**, 602 (1964).
157. Johnston, M. A., and Delwiche, E. A., *J. Bacteriol.* **90**, 347 (1965).
158. Johnston, M. A., and Delwiche, E. A., *J. Bacteriol.* **90**, 352 (1965).
159. Kono, Y., and Fridovich, I., *J. Biol. Chem.* **258**, 6015 (1983).
160. Kono, Y., and Fridovich, I., *J. Bacteriol.* **155**, 742 (1983).
161. Kono, Y., and Fridovich, I., *J. Biol. Chem.* **258**, 13646 (1983).
162. Allgood, G. S., and Perry, J. J., *J. Bacteriol.* **168**, 563 (1986).
163. Barynin, V. V., and Grebenko, A. I., *Dokl. Akad. Nauk SSSR* **286**, 461 (1986).
164. Beyer, W. F., Jr., and Fridovich, I., *Biochemistry* **24**, 6460 (1985).
165. Khangulov, S. V., Barynin, V. V., Melik-Adamyanyan, V. R., Grebenko, A. I., Voevodskaya, N. V., Blyumenfel'd, L. A., Dobryakov, S. N., and Il'yasova, V. B., *Bioorg. Khim.* **12**, 741 (1986).
166. Barynin, V. V., Vagin, A. A., Melik-Adamyanyan, V. R., Grebenko, A. I., Khangulov, S. V., Popov, A. N., Andrianova, M. E., and Vainshtein, B. K., *Dokl. Akad. Nauk SSSR* **288**, 877 (1986).
167. Hendrickson, W. A., Klippenstein, G. L., and Ward, K. B., *Proc. Natl. Acad. Sci. U.S.A.* **72**, 2160 (1975).
168. Sheats, J. E., Czernuszewicz, R. S., Dismukes, G. C., Rheingold, A. L., Petrouleas, V., Stubbe, J., Armstrong, W. H., Beer, R. H., and Lippard, S. J., *J. Am. Chem. Soc.* **109**, 1433 (1987).
169. Wieghardt, K., Bossek, U., Ventur, D., and Weiss, J., *J. Chem. Soc., Chem. Commun.* 347 (1985).
170. Wieghardt, K., Bossek, U., Bonvoisin, J., Beauvillain, P., Girerd, J.-J., Nuber, B., Weiss, J., and Heinze, J., *Angew. Chem., Int. Ed. Engl.* **25**, 1030 (1986).
171. Wieghardt, K., Bossek, U., Zsolna, L., Huttner, G., Blondin, G., Girerd, J.-J., and Babonneau, F., *J. Chem. Soc., Chem. Commun.* 651 (1987).
172. Plaskin, P. M., Stouffer, R. C., Mathew, M., and Palenik, G. J., *J. Am. Chem. Soc.* **94**, 2121 (1972).
173. Scharadt, B. C., Hollander, F. J., and Hill, C. L., *J. Am. Chem. Soc.* **104**, 3964 (1982).
174. Stebler, M., Ludi, A., and Burgi, H.-B., *Inorg. Chem.* **25**, 4743 (1986).
175. Vogt, L. H., Jr., Zalkin, A., and Templeton, D. H., *Inorg. Chem.* **6**, 1725 (1967).
176. Ziolo, R. F., Stanford, R. H., Rossman, G. R., and Gray, H. B., *J. Am. Chem. Soc.* **96**, 7910 (1974).
177. Armstrong, W. H., Spool, A., Papaefthymiou, G. C., Frankel, R. B., and Lippard, S. J., *J. Am. Chem. Soc.* **106**, 3653 (1984); Armstrong, W. H., and Lippard, S. J., *J. Am. Chem. Soc.* **106**, 4632.
178. Wieghardt, K., Pohl, K., and Gebert, W., *Angew. Chem., Int. Ed. Engl.* **22**, 727 (1983); Chaudhuri, P., Wieghardt, K., Nuber, B., and Weiss, J., *Angew. Chem., Int. Ed. Engl.* **24**, 778 (1985).
179. Stenkamp, R. E., Sieker, L. C., Jensen, L. H., McCallum, J. D., and Sanders-Loehr, J., *Proc. Natl. Acad. Sci. U.S.A.* **82**, 713 (1985).
180. Wieghardt, K., Pohl, K., and Ventur, D., *Angew. Chem., Int. Ed. Engl.* **24**, 392 (1985).
181. Wieghardt, K., Bossek, U., Nuber, B., and Weiss, J., *Inorg. Chim. Acta* **126**, 39 (1987).
182. Vincent, J. B., Huffman, J. C., and Christou, G., unpublished results.

183. Bashkin, J. S., Schake, A. R., Vincent, J. B., Chang, H.-R., Li, Q., Huffman, J. C., Christou, G., and Hendrickson, D. N., *J. Chem. Soc., Chem. Commun.* 700 (1988).
184. Pirson, A., *Z. Bot.* **31**, 193 (1937).
185. Amesz, J., *Biochim. Biophys. Acta* **726**, 1 (1983).
186. Kok, B., Forbush, B., and McGloin, M., *Photochem. Photobiol.* **11**, 457 (1970).
187. Wells, C. F., *Nature (London)* **605**, 693 (1965).
188. Kuwabara, T., and Murata, N., *Plant Cell Physiol.* **23**, 533 (1982).
189. Berthold, D. A., Babcock, G. T., and Yocum, C. F., *FEBS Lett.* **134**, 231 (1981).
190. Dunahay, T. G., Staehelin, L. A., Seibert, M., Ogilvie, P. D., and Berg, S. P., *Biochim. Biophys. Acta* **764**, 179 (1984).
191. Murata, N., Miyao, M., Omata, T., Matsunami, H., and Kuwabara, T., *Biochim. Biophys. Acta* **765**, 363 (1984).
192. Yamamoto, Y., Tabata, K., Isogai, Y., Nishimura, M., Okayama, S., Matsuura, K., and Itoh, S., *Biochim. Biophys. Acta* **767**, 493 (1984).
193. Ikeuchi, M., Yuasa, M., and Inoue, Y., *FEBS Lett.* **185**, 316 (1985).
194. Tang, X.-S., and Satoh, K., *FEBS Lett.* **179**, 60 (1985).
195. Ohno, T., Satoh, K., and Katoh, S., *Biochim. Biophys. Acta* **852**, 1 (1986).
196. Kuwabara, T., and Murata, N., *Biochim. Biophys. Acta* **581**, 228 (1979).
197. Abramowicz, D. A., and Dismukes, G. C., *Biochim. Biophys. Acta* **765**, 318 (1984).
198. Yamamoto, Y., Shinkai, H., Isogai, Y., Matsuura, K., and Nishimura, M., *FEBS Lett.* **175**, 429 (1984).
199. Szczepaniak, A., and Hendrich, W., *Biol. Chem. Hoppe-Seyler* **367**, Suppl. 144 (1986).
200. Bowlby, N. R., and Frasch, W. D., *Biochemistry* **25**, 1402 (1986).
201. Oh-oka, H., Tanaka, S., Wada, K., Kuwabara, T., and Murata, N., *FEBS Lett.* **197**, 63 (1986).
202. Miyao, M., and Murata, N., *FEBS Lett.* **170**, 350 (1984).
203. Ono, T.-A., and Inoue, Y., *FEBS Lett.* **168**, 281 (1984).
204. Tang, X.-S., and Satoh, K., *FEBS Lett.* **201**, 221 (1986).
205. Kuwabara, T., Miyao, M., Murata, T., and Murata, N., *Biochim. Biophys. Acta* **806**, 283 (1985).
206. Miyao, M., Murata, N., Lavorel, J., Maison-Petri, B., Boussac, A., and Etienne, A.-L., *Biochim. Biophys. Acta* **890**, 151 (1987).
207. Ono, T.-A., and Inoue, Y., *Biochim. Biophys. Acta* **806**, 331 (1985).
208. Vass, I., Ono, T.-A., and Inoue, Y., *Biochim. Biophys. Acta* **892**, 224 (1987).
209. Miyao, M., and Murata, N., *FEBS Lett.* **164**, 375 (1983).
210. Koike, H., and Inoue, Y., *Biochim. Biophys. Acta* **807**, 64 (1985).
211. Ljungberg, U., Akerlund H.-E., Larson, C., and Andersson, B., *Biochim. Biophys. Acta* **767**, 145 (1984).
212. Murata, N., Miyao, M., and Kuwabara, T., in "The Oxygen Evolving System of Photosynthesis" (Y. Inoue, A. R. Crofts, Govindjee, N. Murata, G. Renger, and K. Satoh, eds.), p. 213. Academic Press, New York, 1983.
213. Isogai, Y., Yamamoto, Y., and Nishimura, M., *FEBS Lett.* **187**, 240 (1985).
214. Irrgang, K.-D., Renger, G., and Vater, J., *FEBS Lett.* **204**, 67 (1986).
215. Metz, J. G., Wong, J., and Bishop, N. I., *FEBS Lett.* **114**, 61 (1980).
216. Metz, J. G., and Seibert, M., *Plant Physiol.* **76**, 829 (1984).
217. Metz, J. G., Bricker, T. M., and Seibert, M., *FEBS Lett.* **185**, 191 (1985).
218. Metz, J. G., Pakrasi, H. B., Seibert, M., and Arntzen, C. J., *FEBS Lett.* **205**, 269 (1986).
219. Kyle, D. J., *Photochem. Photobiol.* **41**, 107 (1985).
220. Vass, J., Ono, T.-A., and Inoue, Y., *FEBS Lett.* **211**, 215 (1987).
221. Ikeuchi, M., and Inoue, Y., *FEBS Lett.* **210**, 71 (1987).
222. Takahashi, Y., Takahashi, M.-A., and Satoh, K., *FEBS Lett.* **208**, 347 (1986).

223. Aoki, K., Ideguchi, T., Kakuno, T., Yamashita, J., and Horio, T., *J. Biochem. Tokyo* **100**, 875 (1986).
224. Alt, J., Morris, J., Westhoff, P., and Herrmann, R. G., *Curr. Gen.* **8**, 597 (1984).
225. Trebst, A., *Z. Naturforsch., C: Biosci.* **41C**, 240 (1986).
226. Deisenhofer, J., Epp, O., Miki, K., Huber, R., and Michel, H., *Nature (London)* **318**, 618 (1985).
227. Geiger, R., Berzborn, R. J., Depka, B., Oettmeier, W., and Trebst, A., *Z. Naturforsch., C: Biosci.* **42C**, 491 (1987).
228. Sayre, R. T., Andersson, B., and Bogorad, L., *Cell (Cambridge, Mass.)* **47**, 601 (1986).
229. Nanba, O., and Satoh, K., *Proc. Natl. Acad. Sci. U.S.A.* **84**, 109 (1987).
230. Danielius, R. V., Satoh, K., van Kan, P. J. M., Plijter, J. J., Nuijs, A. M., and van Gorkum, H. J., *FEBS Lett.* **213**, 241 (1987).
231. Satoh, K., Fujii, Y., Aoshima, T., and Tado, T., *FEBS Lett.* **216**, 7 (1987).
232. Mathur, P., and Dismukes, G. C., *J. Am. Chem. Soc.* **105**, 7093 (1983).
233. Lynch, M. W., Hendrickson, D. N., Fitzgerald, B. J., and Pierpoint, C. G., *J. Am. Chem. Soc.* **106**, 2041 (1984).
234. Takahashi, Y., and Katoh, S., *Biochim. Biophys. Acta* **848**, 183 (1986).
235. Pistorius, E. K., and Gau, A. E., *FEBS Lett.* **206**, 243 (1986).
236. Hanssum, B., Dohnt, G., and Renger, G., *Biochim. Biophys. Acta* **806**, 210 (1985).
237. Dekker, J. P., van Gorkum, H. J., Brok, M., and Ouwehand, L., *Biochim. Biophys. Acta* **764**, 301 (1984).
238. Dekker, J. P., van Gorkum, H. J., Wensink, J., and Ouwehand, L., *Biochim. Biophys. Acta* **767**, 1 (1984).
239. Dekker, J. P., Plijter, J. J., Ouwehand, L., and van Gorkum, H. J., *Biochim. Biophys. Acta* **767**, 176 (1984).
240. Lavergne, J., *Photochem. Photobiol.* **43**, 311 (1986).
241. Renger, G., and Weiss, W., *Biochim. Biophys. Acta* **850**, 184 (1986).
242. Saygin, O., and Witt, H. T., *Photobiochem. Photobiophys.* **10**, 71 (1985).
243. Bodini, M. E., Willis, L. A., Riechel, T. L., and Sawyer, D. T., *Inorg. Chem.* **15**, 1538 (1976).
244. Vincent, J. B., and Christou, G., *FEBS Lett.* **207**, 250 (1986).
245. Witt, H. T., Schlodder, E., Brettel, K., and Saygin, O., *Photosynth. Res.* **9**, 453 (1986).
246. Dismukes, G. C., and Mathis, P., *FEBS Lett.* **178**, 51 (1984); Dismukes, G. C., *Photochem. Photobiol.* **43**, 99 (1986).
247. Cole, J., and Sauer, K., *Biochim. Biophys. Acta* **891**, 40 (1987).
248. Forster, V., Hong, Y.-Q., and Junge, W., *Biochim. Biophys. Acta* **638**, 141 (1981).
249. Cooper, S. R., and Calvin, M., *J. Am. Chem. Soc.* **99**, 6623 (1977).
250. Yachandra, V. K., Guiles, R. D., McDermott, A., Britt, R. D., Dexheimer, S. L., Sauer, K., and Klein, M. P., *Biochim. Biophys. Acta* **850**, 324 (1986).
251. Yachandra, V. K., Guiles, R. D., McDermott, A., Cole, J., Britt, R. D., Dexheimer, S. L., Sauer, K., and Klein, M. P., *Prog. Photosynth. Res., Proc. Int. Congr. Photosynth., 7th, 1987*, Vol. 1, p. 557 (1987).
252. McDermott, A., Yachandra, V. K., Guiles, R. D., Britt, R. D., Dexheimer, S. L., Sauer, K., and Klein, M. P., *Prog. Photosynth. Res., Proc. Int. Congr. Photosynth., 7th, 1987*, Vol. 1, p. 565 (1987).
253. Guiles, R. D., Yachandra, V. K., McDermott, A. E., Britt, R. D., Dexheimer, S. L., Sauer, K., and Klein, M. P., *Prog. Photosynth. Res., Proc. Int. Congr. Photosynth., 7th, 1987*, Vol. 1, p. 561 (1987).
254. Goodin, D. B., Yachandra, J. K., Britt, D., Sauer, K., and Klein, M. P., *Biochim. Biophys. Acta* **767**, 209 (1984).
255. Dismukes, G. C., and Siderer, Y., *FEBS Lett.* **121**, 78 (1980).

256. Dismukes, G. C., and Siderer, Y., *Proc. Natl. Acad. Sci. U.S.A.* **78**, 274 (1981).
257. Dismukes, G. C., Ferris, K., and Watnick, P., *Photobiochem. Photobiophys.* **3**, 243 (1982).
258. Dismukes, G. C., Abramowicz, D. A., Ferris, K. F., Mathur, P., Siderer, Y., Upadrashta, B., and Watnick, P., in "The Oxygen Evolving System of Photosynthesis" (Y. Inoue, A. R. Croft, Govindjee, N. Murata, G. Renger, and K. Satoh, eds.), p. 145. Academic Press, New York, 1983.
259. Casey, J. L., and Sauer, K., *Biochim. Biophys. Acta* **767**, 21 (1984).
260. Cole, J., Yachandra, V. K., Guiles, R. D., McDermott, A. E., Britt, R. D., Dexheimer, S. L., Sauer, K., and Klein, M. P., *Biochim. Biophys. Acta* **890**, 395 (1987).
261. Rutherford, A. W., *Biochim. Biophys. Acta* **807**, 189 (1985).
262. Beck, W. F., de Paula, J. C., and Brudvig, G. W., *Biochemistry* **24**, 3035 (1985).
263. Zimmermann, J.-L., and Rutherford, A. W., *Biochemistry* **25**, 4609 (1986).
264. de Paula, J. C., Innes, J. B., and Brudvig, G. W., *Biochemistry* **24**, 8114 (1985).
265. Hansson, O., Andreasson, L.-E., and Vanngard, T., *Adv. Photosynth. Res.* **1**, 307 (1984).
266. Dismukes, G. C., and Damoder, R., *Biophys. J.* **47**, 166a (1985).
267. de Paula, J. C., and Brudvig, G. W., *J. Am. Chem. Soc.* **107**, 2643 (1985).
268. de Paula, J. C., Beck, W. F., and Brudvig, G. W., *J. Am. Chem. Soc.* **108**, 4002 (1986).
269. Hansson, O., Aasa, R., and Vanngard, T., *Biophys. J.* **51**, 825 (1987).
270. Dismukes, G. C., *Photochem. Photobiol.* **45**, 3S (1987).
271. Hansson, O., Andreasson, L.-E., and Vanngard, T., *FEBS Lett.* **195**, 151 (1986).
272. Yachandra, V. K., Guiles, R. D., Sauer, K., and Klein, M. P., *Biochim. Biophys. Acta* **850**, 333 (1986).
273. Klein, M. P., *Photochem. Photobiol.* **45**, 4S (1987).
274. Velthuys, B. R., *Biochim. Biophys. Acta* **396**, 392 (1975).
275. Beck, W. F., and Brudvig, G. W., *Biochemistry* **25**, 6479 (1986).
276. Beck, W. F., de Paula, J. C., and Brudvig, G. W., *J. Am. Chem. Soc.* **108**, 4018 (1986).
277. Britt, R. D., Sauer, K., and Klein, M. P., *Prog. Photosynth. Res., Proc. Int. Congr. Photosyn., 7th, 1987*, Vol. 1, p. 573 (1987).
278. de Groot, A., Plijter, J. J., Evelo, R., Babcock, G. T., and Hoff, A. J., *Biochim. Biophys. Acta* **848**, 8 (1986).
279. Styring, S., and Rutherford, A. W., *Biochemistry* **26**, 2401 (1987).
280. Hunziker, D., Abramowicz, D. A., Damoder, R., and Dismukes, G. C., *Biochim. Biophys. Acta* **890**, 6 (1987).
281. Srinivasan, A. H., and Sharp, R. R., *Biochim. Biophys. Acta* **850**, 211 (1986).
282. Srinivasan, A. H., and Sharp, R. R., *Biochim. Biophys. Acta* **851**, 369 (1986).
283. Tamura, N., and Cheniae, G. M., *FEBS Lett.* **200**, 231 (1986).
284. Velthuys, B., and Kok B., *Biochim. Biophys. Acta* **502**, 211 (1978).
285. Radmer, R., and Ollinger, O., *FEBS Lett.* **144**, 162 (1982).
286. Mano, J., Takahashi, M.-A., and Asada, K., *Biochemistry* **26**, 2495 (1987).
287. Frasch, W. D., and Mei, R., *Biochim. Biophys. Acta* **891**, 8 (1987).
288. Schmid, G. H., and Thibault, P., *Z. Naturforsch., C: Biosci.* **38C**, 60 (1983).
289. Bader, K. P., Thibault, P., and Schmid, G. H., *Z. Naturforsch., C: Biosci.* **38C**, 778 (1983).
290. Pistorious, E. K., and Schmid, G. H., *Biochim. Biophys. Acta* **890**, 352 (1987).
291. Forster, V., and Junge, W., *Photochem. Photobiol.* **41**, 183 (1985).
292. Forster, V., and Junge, W., *Photochem. Photobiol.* **41**, 191 (1985).
293. Forster, V., and Junge, W., *FEBS Lett.* **186**, 153 (1985).
294. Radmer, R., and Ollinger, O., *FEBS Lett.* **195**, 285 (1986).
295. Krishtalik, L. I., *Biochim. Biophys. Acta* **849**, 162 (1986).
296. Saygin, O., and Witt, H. T., *FEBS Lett.* **176**, 83 (1984).
297. Saygin, O., and Witt, H. T., *FEBS Lett.* **187**, 224 (1985).
298. Dekker, J. P., and van Gorkum, H. J., *J. Bioenerg. Biomembr.* **19**, 125 (1987).

299. Sumner, C. E., Jr., and Steinmetz, G. R., *J. Am. Chem. Soc.* **107**, 6124 (1985).
300. Saygin, O., Gerken, S., Meyer, B., and Witt, H. T., *Photosynth. Res.* **9**, 71 (1986).
301. Baikie, A. R. E., Hursthouse, M. B., New, D. B., and Thornton, P., *J. Chem. Soc., Chem. Commun.* 62 (1978).
302. Baikie, A. R. E., Hursthouse, M. B., New, L., Thornton, D., and White, R. G., *J. Chem. Soc., Chem. Commun.* 684 (1980).
303. Vincent, J. B., Chang, H.-R., Folting, K., Huffman, J. C., Christou, G., and Hendrickson, D. N., *J. Am. Chem. Soc.* **109**, 5703 (1987).
304. Vincent, J. B., and Christou, G., *Inorg. Chim. Acta* **136**, L41 (1987).
305. Hessel, L. W., and Romers, C., *Recl. Trav. Chim. Pays-Bas* **88**, 545 (1969).
306. Lis, T., and Jezowska-Trezebiatowska, B., *Acta Crystallogr., Sect. B* **B3**, 2112 (1977).
307. Wieghardt, K., Bossek, U., and Gebert, W., *Angew. Chem., Int. Ed. Engl.* **22**, 328 (1983).
308. Vincent, J. B., Christmas, C., Huffman, J. C., Christou, G., Chang, H.-R., and Hendrickson, D. N., *J. Chem. Soc., Chem. Commun.* 236 (1987).
309. Christmas, C., Vincent, J. B., Huffman, J. C., Christou, G., Chang, H.-R., and Hendrickson, D. N., *J. Chem. Soc., Chem. Commun.* 1303 (1987).
310. Bashkin, J. S., Chang, H.-R., Streib, W. E., Huffman, J. C., Hendrickson, D. N., and Christou, G., *J. Am. Chem. Soc.* **109**, 6502 (1987).
311. Baikie, A. R. E., Howes, A. J., Hursthouse, M. B., Quick, A. B., and Thornton, P., *J. Chem. Soc., Chem. Commun.* 1587 (1986).
312. Kirby, J. A., Robertson, A. S., Smith, J. P., Thompson, A. C., Cooper, S. R., and Klein, M. P., *J. Am. Chem. Soc.* **103**, 5529 (1981).
313. Klein, M. P., *Photochem. Photobiol.* **45**, 45 (1987).
314. Cooper, S. R., Dismukes, G. C., Klein, M. P., and Calvin, M., *J. Am. Chem. Soc.* **100**, 7248 (1978).
315. Dismukes, G. C., and Damoder, R., *Biophys. J.* **47**, 166a (1985).
316. Coleman, W. M., and Taylor, L. T., *Coord. Chem. Rev.* **32**, 1 (1980).
317. Boreham, C. J., and Chiswell, B., *Inorg. Chim. Acta* **24**, 77 (1977).
318. Vincent, J. B., Christmas, C., Chang, H.-R., Li, Q., Boyd, P. D. W., Huffman, J. C., Hendrickson, D. N., and Christou, G., *J. Am. Chem. Soc.*, in press (1989).
319. Christmas, C., Vincent, J. B., Huffman, J. C., Christou, G., Chang, H.-R., and Hendrickson, D. N., *Angew. Chem., Int. Ed. Engl.* **26**, 915 (1987).
320. Christmas, C., Vincent, J. B., Chang, H.-R., Huffman, J. C., Christou, G., and Hendrickson, D. N., *J. Am. Chem. Soc.* **110**, 823 (1988).
321. Lis, T., *Acta Crystallogr., Sect. B* **B36**, 2042 (1980).
322. Boyd, P. D. W., Li, Q., Vincent, J. B., Folting, K., Chang, H.-R., Streib, W. E., Huffman, J. C., Christou, G., and Hendrickson, D. N., *J. Am. Chem. Soc.* **110**, 8537 (1988).
323. Klein, M. P., personal communication (1987).
324. Padhye, S., Kambara, T., Hendrickson, D. N., and Govindjee, *Photosynth. Res.* **9**, 103 (1986).
325. Li, Q., Vincent, J. B., Libby, E., Chang, H.-R., Huffman, J. C., Christou, G., and Hendrickson, D. N., *Angew. Chem. Int. Ed. Engl.*, in press (1989).
326. Brudvig, G. W., and Crabtree, R. H., *Proc. Natl. Acad. Sci. U.S.A.* **83**, 4586 (1986).
327. Archibald, F., *Crit. Rev. Microbiol.* **13**, 63 (1986); McEven, A. R., *Inorg. Biochem.* **2**, 249 (1979); Lawrence, G. D., and Sawyer, D. T., *Coord. Chem. Rev.* **27**, 173 (1978).

---

In recent work, the existence of a Mn acid phosphatase has been questioned (84). There is now substantial evidence for a binuclear Mn ribonucleotide reductase [Willing, A., Follmann, H., and Auling, G., *Eur. J. Biochem.* **170**, 603 (1988) and **175**, 167 (1988)], and the models discussed are relevant also to this class of enzyme.